Directional Wavelet Bases Construction on Dyadic Quincunx Lattice

Rujie Yin, Ingrid Daubechies

April 6, 2016

Abstract

We construct directional wavelet systems that have the same direction selectivity as shearlets in the first frequency dyadic ring and non-uniform directional wavelet filterbanks(nuDFB). In particular, dilated quincunx downsampling is used to construct orthonormal and bi-orthogonal bases and standard dyadic downsampling for low-redundancy frames. We prove that the support of orthonormal and bi-orthogonal wavelets is discontinuous in the frequency domain, which can be avoided in frames of redundancy as low as 2. These are the first step towards the construction of efficient shearlet systems.

1   Introduction

In image compression and analysis, 2D tensor wavelet schemes are widely used. Despite the time-frequency localization inherited from 1D wavelet, 2D tensor wavelets suffers from poor orientation selectivity: only horizontal or vertical edges are well represented by tensor wavelets. To obtain better representation of 2D images, several directional wavelet schemes have been proposed and applied to image processing, including directional wavelet filterbanks(DFB), contourlet, curvelet, shearlet and dual-tree wavelet.

Conventional DFB [1] divides the frequency domain into eight equi-angular pairs of triangles and it is critically downsampled (maximally decimated) and perfect reconstruction (PR), but without multi-resolution structure. A non-uniform DFB(nuDFB) is introduced in [2] where the high frequency ring is divided into six equi-angular pairs of trapezoids and the central low frequency square is kept for division in the next level of decomposition. The nuDFB is solved directly by optimization which provides a non-unique near orthogonal or bi-orthogonal solution depending on the initialization. Contourlets [3] combine the Laplacian pyramid scheme with DFB which has PR but with redundancy 4/3 inherited from the Laplacian pyramid. Shearlet [4, 5] and curvelet [6] systems construct a multi-resolution partition of the frequency domain by applying shear or rotation operators to a generator function in each level. Depending on the generator function and the number of directions, available shearlet and curvelet

implementations have redundancy at least 4; moreover, the factor may grow with the decomposition level. Dual-tree wavelets [7] are linear combinations of 2D tensor wavelets (corresponding to multi-resolution systems) that constitute an approximate Hilbert transform pair.

None of these schemes is PR, critically downsampled and regularized (localized in both time and frequency) with multi-resolution structure. In the framework of nuDFB ([2]), it is shown by Durand [8] that it's impossible to construct orthonormal filters localized in frequency without discontinuity in their frequency support, or equivalently regularized filters without aliasing. His construction of directional filters using compositions of 2-band filters associated to quincunx lattice, similar to that of uniform DFB in [2] and as pointed out in [2] the overall composed filters are not alias-free.

In this paper, we consider multi-resolution directional wavelets corresponding to the same partition of frequency domain as nuDFB and build a framework to analyze the equivalent conditions of PR for critically downsampled and more generally redundant schemes. In our previous work [9], we show that in multi-resolution analysis(MRA), PR is equivalent to an identity condition and shift-cancellation condition closely related to the frequency support of filters and their downsampling scheme. Based on these two conditions, we derive Durand's discontinuity result of orthonormal schemes and a relaxation of orthonormal schemes to frame with redundancy 2 that resolves the regularity limitation. A regularized directional wavelet scheme of redundancy 2 that satisfies the identity condition and the relaxed shift-cancellation condition, is constructed directly by smoothing the Fourier transform of the corresponding wavelet. We extend our previous work here and show that the same irregularity in orthonormal schemes exists in bi-orthogonal schemes. Our analysis of bi-orthogonal schemes is based on a numerical algorithm introduced by Cohen et al in [10] for constructing compactly supported symmetric wavelet bases on hexagonal lattice. We extend and adapt this algorithm to our bi-orthogonal framework.

The paper is organized as follows, in section 2, we set up our framework of a dyadic MRA with dilated quincunx downsampling. In section 3, we review the irregularity of orthonormal schemes in [9]. In particular, we derive two conditions, *identity summation* and *shift cancellation*, equivalent to perfect reconstruction in this MRA with critical downsampling. These lead to the classification of *regular/singular* boundaries of the frequency partition and a *relaxed shift-cancellation* condition for low-redundancy MRA frame allows better regularity of the directional wavelets. In section 4, we show the irregularity for bi-orthogonal schemes. We first review the wavelet construction algorithm in [10] which solves linear systems generated from regularity constraints. Next, we extend the algorithm to our framework and show that the resulting linear system doesn't have feasible solution satisfying all regularity constraints, especially continuity of Fourier transforms of wavelet filters. Finally, we conclude our results and discuss future work in section 7.

2 Framework Setup

We summarize 2D-MRA systems and the relation between frequency domain partition and sub-lattice of $\mathbb{Z}^2$ with critical downsampling following [9].

2.1 Notation

Throughout this paper, we use lower case normal font for function, normal font for scalar, upper case bold font for matrix, lower case bold font for vector and upper case normal font for frequency domain.

2.2 Multi-resolution analysis and sub-lattice sampling

In an MRA, given a scaling function $\phi \in L^2(\mathbb{R}^2)$, s.t. $\|\phi\|_2 = 1$, the base approximation space is defined as $V_0 = \overline{span\{\phi_{0,\boldsymbol{k}}\}}_{\boldsymbol{k}\in\mathbb{Z}^2}$, where $\phi_{0,\boldsymbol{k}} = \phi(\boldsymbol{x} - \boldsymbol{k})$. If $\langle\phi_{0,\boldsymbol{k}},\phi_{0,\boldsymbol{k}'}\rangle = \delta_{\boldsymbol{k},\boldsymbol{k}'}$, then $\{\phi_{0,\boldsymbol{k}}\}$ is an orthonormal basis of V_0. In addition, ϕ is associated with a scaling matrix $\mathbf{D} \in \mathbb{Z}^{2\times2}$, s.t. the dilated scaling function $\phi_1(\boldsymbol{x}) = |\mathbf{D}|^{-1/2}\phi(\mathbf{D}^{-1}\boldsymbol{x})$ is a linear combination of $\phi_{0,\boldsymbol{k}}$. Equivalently, $\exists m_0(\boldsymbol{\omega}) = m_0(\omega_1,\omega_2)$, $2\pi-$periodic in ω_1,ω_2, s.t. in the frequency domain

$$\widehat{\phi}(\mathbf{D}^T\boldsymbol{\omega}) = m_0(\boldsymbol{\omega})\widehat{\phi}(\boldsymbol{\omega}). \tag{1}$$

Hence

$$\hat{\phi}(\boldsymbol{\omega}) = (2\pi)^{-1}\prod_{k=1}^{\infty}m_0(\mathbf{D}^{-k}\boldsymbol{\omega}). \tag{2}$$

Define the nested approximation spaces $V_l = \overline{span\{\phi(\mathbf{D}^{-l}\boldsymbol{x} - \boldsymbol{k}); \boldsymbol{k} \in \mathbb{Z}^2\}}$, $l \in \mathbb{Z}$ and W_l as the orthogonal complement of V_l with respect to V_{l-1} in MRA. Suppose there are J wavelet functions $\psi^j \in L^2(\mathbb{R}^2)$, $1 \le j \le J$, and $\mathbf{Q} \in \mathbb{Z}^{2\times2}$, s.t.

$$W_1 = \bigcup_{j=1}^{J}W_1^j = \bigcup_{j=1}^{J}\overline{span\{\psi_{1,\boldsymbol{k}}^j; \boldsymbol{k} \in \mathbf{Q}\mathbb{Z}^2\}} = \bigcup_{j=1}^{J}\overline{span\{\psi^j(\mathbf{D}^{-1}\boldsymbol{x} - \boldsymbol{k}); \boldsymbol{k} \in \mathbf{Q}\mathbb{Z}^2\}}.$$

An L-level multi-resolution system with base space V_0 is then spanned by

$$\{\phi_{L,\boldsymbol{k}}, \psi_{l,\boldsymbol{k}'}^j, 1 \le l \le L, \boldsymbol{k} \in \mathbb{Z}^2, \boldsymbol{k}' \in \mathbf{Q}\mathbb{Z}^2, 1 \le j \le J\}. \tag{3}$$

In particular, we set $\mathbf{D} = \mathbf{D_2} \doteq \left(\begin{smallmatrix}2&0\\0&2\end{smallmatrix}\right)$ and $\mathbf{Q} := \left(\begin{smallmatrix}1&1\\-1&1\end{smallmatrix}\right)$. As $W_1 \subset V_0$, each rescaled wavelet $\psi^j(\mathbf{D}^{-1}\cdot)$ is also a linear combination of $\phi_{0,\boldsymbol{k}}$, so that $\exists m_j$ analogous to m_0 satisfying

$$\widehat{\psi^j}(\mathbf{D}^T\boldsymbol{\omega}) = m_j(\boldsymbol{\omega})\widehat{\phi}(\boldsymbol{\omega}), \qquad 1 \le j \le J. \tag{4}$$

In this construction of MRA, the corresponding subsampling matrix of $\phi_{1,\boldsymbol{k}}$ is $\mathbf{D}$ and that of $\psi_{1,\boldsymbol{k}}^j$ is $\mathbf{QD}$, the dilated quincunx subsample (see the right panel in Fig.1), as in [8].

2.3 Frequency domain partition and critical downsampling

Consider the canonical frequency square, $S_0 = [-\pi,\pi) \times [-\pi,\pi)$ associated with lattice $\mathcal{L} = \mathbb{Z}^2$. If C_j are the main support of m_j, $0 \le j \le J$, then due to
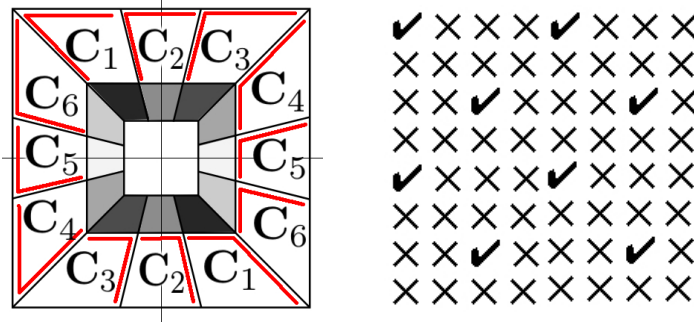
Figure 1: Left: partition of S_0 and boundary assignment of C_j, $j = 1, \cdots, 6$ (each C_j has boundaries indicated by red line segments), Right: dilated quincunx sub-lattice.

(1) and (4) they form a partition of S_0. To build an orthonormal basis with good directional selectivity, we choose the partition of S_0 to be that of the least redundant shearlet system, see Fig.1 left, which is also Example B in [8]. In this partition, S_0 is divided into a central square $C_0 = S_1 := \left(\begin{smallmatrix} 2 & 0 \\ 0 & 2 \end{smallmatrix} \right)^{-1} S_0$ and a ring: the ring is further cut into six pairs of directional trapezoids C_j's by lines passing through the origin with slopes $\pm 1, \pm 3$ and $\pm \frac{1}{3}$. The central square S_1 can be further partitioned in the same way to obtain a two-level multi-resolution system, as shown in Fig.1.

Here $J = 6$ and $|\mathbf{D}|^{-1} + J |\mathbf{Q}\mathbf{D}|^{-1} = 1/4 + 6/(2 \cdot 4) = 1$, hence the corresponding MRA generated by (3) achieves critical downsampling([8]). Furthermore, let $\boldsymbol{\pi}_0 = (0,0), \boldsymbol{\pi}_1 = (\pi/2, \pi/2), \boldsymbol{\pi}_2 = (\pi, 0), \boldsymbol{\pi}_3 = (-\pi/2, \pi/2), \boldsymbol{\pi}_4 = (0, \pi), \boldsymbol{\pi}_5 = (\pi/2, -\pi/2), \boldsymbol{\pi}_6 = (\pi, \pi), \boldsymbol{\pi}_7 = (-\pi/2, -\pi/2)$, then each piece C_j together with its shifts form a tiling of S_0, i.e.

$$S_0 = \bigcup_{\boldsymbol{\pi} \in \Gamma_0} (C_j + \boldsymbol{\pi}) = \bigcup_{\boldsymbol{\pi} \in \Gamma_1} (C_0 + \boldsymbol{\pi}), \quad j = 1, \cdots, 6 \tag{5}$$

where $\Gamma_0 = \{\boldsymbol{\pi}_i, i = 0, 2, 4, 6\}$ and $\Gamma_1 = \{\boldsymbol{\pi}_i, i = 0, \cdots, 7\}$.

3 Orthonormal Bases

In this section, we discuss the conditions on $m-$ functions such that the corresponding MRA forms an orthonormal bases.

We begin with the two key conditions, i.e. *identity summation* and *shift cancellation*, on $m-$functions such that the system (3) is perfect reconstruction (PR) or equivalently a Parseval frame in MRA.

3.1 orthonormal conditions on $m-$functions

In MRA, (3) is PR if $\forall f \in L_2(\mathbb{R}^2)$,

$$\sum_k \langle f, \phi_{0,k} \rangle \phi_{0,k} = \sum_k \langle f, \phi_{1,k} \rangle \phi_{1,k} + \sum_j \sum_k \langle f, \psi_{1,k}^j \rangle \psi_{1,k}^j. \tag{6}$$

4

Using (1) and (4) together with the admissibility of the frequency partition, this condition on ϕ and ψ^j's yields:

Theorem 1. *The perfect reconstruction condition holds for* (3) *iff the following two conditions hold*

$$|m_0(\boldsymbol{\omega})|^2 + \sum_{j=1}^{6} |m_j(\boldsymbol{\omega})|^2 = 1 \tag{7}$$

$$\begin{cases} \sum_{j=0}^{6} m_j(\boldsymbol{\omega})\overline{m_j(\boldsymbol{\omega}+\boldsymbol{\pi})} = 0, & \boldsymbol{\pi} \in \Gamma_0 \setminus \{\mathbf{0}\} \\ \sum_{j=1}^{6} m_j(\boldsymbol{\omega})\overline{m_j(\boldsymbol{\omega}+\boldsymbol{\pi})} = 0, & \boldsymbol{\pi} \in \Gamma_1 \setminus \Gamma_0 \end{cases} \tag{8}$$

Theorem 1 is a corollary of Prop. 1 and Prop. 2 in [8]. We give an alternate proof in Appendix A. In Theorem 1, Eq. (7) is the *identity summation* condition, guaranteeing conservation of l_2 energy; Eq. (8) is the *shift cancellation* condition such that aliasing is canceled correctly in reconstruction.

For (3) to be an orthonormal basis, $\{\phi_{\boldsymbol{k}}\}_{\boldsymbol{k}\in\mathbb{Z}^2}$ need to be an orthonormal basis, which is determined by m_0 in (2). In 1D MRA, Cohen's theorem in [11] provides a necessary and sufficient condition on m_0 such that (3) is an orthonormal basis. We generalized this theorem to 2D in [9].

Theorem 2. *Assume that m_0 is a trigonometric polynomial with $m_0(0) = 1$, and define $\hat{\phi}(\boldsymbol{\omega})$ as in* (2).
If $\phi(\cdot - \boldsymbol{k}), \boldsymbol{k} \in \mathbb{Z}^2$ are orthonormal, then $\exists K$ containing a neighborhood of 0, s.t. $\forall \boldsymbol{\omega} \in S_0$, $\boldsymbol{\omega}+2\pi\mathbf{n} \in K$ for some $\mathbf{n} \in \mathbb{Z}^2$, and $\inf_{k>0,\,\boldsymbol{\omega}\in K} |m_0(\mathbf{D_2}^{-k}\boldsymbol{\omega})| > 0$. Further, if $\sum_{\boldsymbol{\pi}\in\Gamma_0} |m_0(\boldsymbol{\omega}+\boldsymbol{\pi})|^2 = 1$, then the inverse is true.

3.2 m-function Design and Boundary Regularity

Let each m_j be an indicator function, $m_0 = \mathbb{1}_{S_1}$, $m_j = \mathbb{1}_{C_j}$, $1 \le j \le 6$, and we use the boundary assignment of C_j in Fig.1, then the identity summation follows from the frequency partition, and the shift cancellation follows from (5).Applying Theorem 2 to m_0, we check that the Shannon-type wavelets generated from these $m-$functions form an orthonormal basis.

In order to improve their spatial localization, m_j need to be regularized, or equivalently, the discontinuity of m_j on ∂C_j, the boundaries of C_j, need to be smoothed. As shown in Proposition 3 in [8], it is not possible to smooth all the discontinuous boundaries if m_j satisfy the perfect reconstruction condition. In [9], ∂C_j are segmented into *singular* and *regular* pieces. On those *singular* pieces, it is shown that m_j cannot be smoothed without violating the shift cancellation condition. Yet, on regular boundaries, m_j can be smoothed in a coherent way such that all the constraints are satisfied. Fig. 2 shows the boundary classification, where the corners of S_0 and S_1 are singular, hence m_0 and the diagonal $m-$ functions of an orthonormal bases are discontinuous there. A mechanism of constructing orthonormal bases by smoothing m_j on regular boundaries from indicator functions is provided in [9].

Figure 2: Boundary classification, singular (red) and regular (yellow)

3.3 Extension to low-redundancy tight frame

The irregularity of orthonormal bases is overcome in the following low-redundancy tight frame construction,

$$\{\phi_{L,\boldsymbol{k}}, \psi^j_{l,\boldsymbol{k'}}, 1 \le l \le L, \boldsymbol{k}, \boldsymbol{k'} \in \mathbb{Z}^2, 1 \le j \le J\}. \tag{9}$$

where all wavelet coefficients are sub-sampled on dyadic sub-lattice and any $L-$level MRA frame doesn't exceed $\frac{J/|D|}{1-1/|D|} = \frac{6/4}{1-1/4} = 2$. We have now

Theorem 3. *The perfect reconstruction condition holds for* (9) *iff the following both hold*

$$|m_0(\boldsymbol{\omega})|^2 + \sum_{j=1}^{6} |m_j(\boldsymbol{\omega})|^2 = 1 \tag{10}$$

$$\sum_{j=0}^{6} m_j(\boldsymbol{\omega})\overline{m_j(\boldsymbol{\omega} + \boldsymbol{\pi})} = 0, \quad \boldsymbol{\pi} \in \Gamma_0 \setminus \{\boldsymbol{0}\} \tag{11}$$

Theorem 3 can be proved analogously to Theorem 1, with fewer shift cancellation constraints now. Following the same analysis of boundary regularity as previous, we show in [9] that all boundaries can be smoothed properly and we obtained directional wavelets with much better spatial and frequency localization than the one constructed by Durand in [8].

Heretofore, we have considered two directional wavelet MRA systems (3) and (9) such that the directional wavelets characterize 2D signals in six equi-angled directions. Furthermore, these wavelets are well localized in the frequency domain such that $supp(m_j)$ is convex and $\exists \epsilon \, s.t.$

$$\sup_{\boldsymbol{\omega'} \in supp(m_j)} \inf_{\boldsymbol{\omega} \in C_j} \|\boldsymbol{\omega'} - \boldsymbol{\omega}\| < \epsilon, \quad 0 \le j \le 6. \tag{12}$$

This desirable condition is hard to obtain by multi-directional filter bank assembly of several elementary filter banks.

In the next section, we analyze the more general case of directional bi-orthorgonal filters constructed with respect to the same frequency partition.

4 Bi-orthogonal Bases

In this section, we analyze the bi-orthogonal bases $\{\phi_{L,\boldsymbol{k}}, \widetilde{\phi}_{L,\boldsymbol{k}}, \psi_{l,\boldsymbol{k}}, \widetilde{\psi}_{l,\boldsymbol{k}}, 1 \le l \le L, \boldsymbol{k} \in \mathbb{Z}^2, 1 \le j \le J\}$, where ϕ, ψ satisfy (1) and (4), and $\widetilde{\phi}, \widetilde{\psi}$ satisfy the

same MRA,

$$\widehat{\widetilde{\phi}}(\boldsymbol{D}^T\boldsymbol{\omega}) = \widetilde{m_0}(\boldsymbol{\omega})\widehat{\widetilde{\phi}}(\boldsymbol{\omega}), \quad \widehat{\widetilde{\phi}}(\boldsymbol{D}^T\boldsymbol{\omega}) = \widetilde{m_0}(\boldsymbol{\omega})\widehat{\widetilde{\phi}}(\boldsymbol{\omega}).$$

For bi-orthogonal bases, we have the similar identity summation and shift cancellation condition to Theorem 1.

Theorem 4. *The perfect reconstruction iff the following two conditions hold*

$$m_0(\boldsymbol{\omega})\overline{\widetilde{m_0}}(\boldsymbol{\omega}) + \sum_{j=1}^{6} m_j(\boldsymbol{\omega})\overline{\widetilde{m_j}}(\boldsymbol{\omega}) = 1 \tag{13}$$

$$\begin{cases} \sum_{j=0}^{6} m_j(\boldsymbol{\omega})\overline{\widetilde{m_j}}(\boldsymbol{\omega} + \boldsymbol{\pi}) = 0, & \boldsymbol{\pi} \in \Gamma_0 \setminus \{\boldsymbol{0}\} \\ \sum_{j=1}^{6} m_j(\boldsymbol{\omega})\overline{\widetilde{m_j}}(\boldsymbol{\omega} + \boldsymbol{\pi}) = 0, & \boldsymbol{\pi} \in \Gamma_1 \setminus \Gamma_0 \end{cases} \tag{14}$$

The conditions (13) and (14) can be combined into a linear system as follows,

$$\begin{bmatrix} \overline{\widetilde{m_0}}(\boldsymbol{\omega}) & \overline{\widetilde{m_1}}(\boldsymbol{\omega}) & \dots & \overline{\widetilde{m_6}}(\boldsymbol{\omega}) \\ 0 & \overline{\widetilde{m_1}}(\boldsymbol{\omega}+\boldsymbol{\pi}_1) & \dots & \overline{\widetilde{m_6}}(\boldsymbol{\omega}+\boldsymbol{\pi}_1) \\ \overline{\widetilde{m_0}}(\boldsymbol{\omega}+\boldsymbol{\pi}_2) & \overline{\widetilde{m_1}}(\boldsymbol{\omega}+\boldsymbol{\pi}_2) & \dots & \overline{\widetilde{m_6}}(\boldsymbol{\omega}+\boldsymbol{\pi}_2) \\ \vdots & \vdots & \vdots & \vdots \\ 0 & \overline{\widetilde{m_1}}(\boldsymbol{\omega}+\boldsymbol{\pi}_7) & \dots & \overline{\widetilde{m_6}}(\boldsymbol{\omega}+\boldsymbol{\pi}_7) \end{bmatrix} \begin{bmatrix} m_0(\boldsymbol{\omega}) \\ m_1(\boldsymbol{\omega}) \\ m_2(\boldsymbol{\omega}) \\ \vdots \\ m_6(\boldsymbol{\omega}) \end{bmatrix} = \begin{bmatrix} 1 \\ 0 \\ 0 \\ \vdots \\ 0 \end{bmatrix} \tag{15}$$

In addition, the orthogonal condition on $m_j, \widetilde{m_j}$ is an analogue of Theorem 2.

Theorem 5. *Assume that $m_0, \widetilde{m_0}$ are trigonometric polynomials with $m_0(0) = \widetilde{m_0}(0) = 1$, which generate $\phi, \widetilde{\phi}$ respectively.*
If $\phi(\cdot - \boldsymbol{k}), \widetilde{\phi}(\cdot - \boldsymbol{k})\boldsymbol{k} \in \mathbb{Z}^2$ are bi-orthogonal, then $\exists K$ containing a neighborhood of 0, s.t. $\forall \boldsymbol{\omega} \in S_0, \boldsymbol{\omega}+2\pi\mathbf{n} \in K$ for some $\mathbf{n} \in \mathbb{Z}^2$, and $\inf_{k>0, \boldsymbol{\omega} \in K} |m_0(\mathbf{D_2}^{-k}\boldsymbol{\omega})| > 0, \inf_{k>0, \boldsymbol{\omega} \in K} |\widetilde{m_0}(\mathbf{D_2}^{-k}\boldsymbol{\omega})| > 0$. Further, if $\sum_{\boldsymbol{\pi} \in \Gamma_0} m_0(\boldsymbol{\omega} + \boldsymbol{\pi})\overline{\widetilde{m_0}}(\boldsymbol{\omega} + \boldsymbol{\pi}) = 1$, then the inverse is true.

By Theorem 5, the linear system (15) of a bi-orthogonal basis need to satisfy the following identity constraint on m_0 and $\widetilde{m_0}$,

$$m_0\overline{\widetilde{m_0}}(\boldsymbol{\omega}) + m_0\overline{\widetilde{m_0}}(\boldsymbol{\omega}+\boldsymbol{\pi}_2) + m_0\overline{\widetilde{m_0}}(\boldsymbol{\omega}+\boldsymbol{\pi}_4) + m_0\overline{\widetilde{m_0}}(\boldsymbol{\omega}+\boldsymbol{\pi}_6) = 1. \tag{16}$$

We thus consider feasible solutions of (15) with constraint (16) using the same approach in [10], which solves compactly supported symmetric bi-orthogonal filters on hexagon lattice. We next review the main scheme in [10] and extend it to our setup of directional wavelet filter.

4.1 Summary of Cohen et al's construction

We summerize the main setup and the approach in [10]. Consider a bi-orthogonal scheme consists of 3 high-pass filters m_1, m_2 and m_3 and a low-pass filter m_0 together with their bi-orthogonal duals $\widetilde{m_j}$, s.t. m_0 is $\frac{2\pi}{3}$-rotation invariant and m_1, m_2, m_3 are $\frac{2\pi}{3}$-rotation co-variant.

This bi-orthogonal scheme satisfies the following linear system (Lemma 2.2.2

in [10])

$$
\begin{bmatrix}
\overline{\widetilde{m_0}(\boldsymbol{\omega})} & \overline{\widetilde{m_1}(\boldsymbol{\omega})} & \overline{\widetilde{m_2}(\boldsymbol{\omega})} & \overline{\widetilde{m_3}(\boldsymbol{\omega})} \\
\overline{\widetilde{m_0}(\boldsymbol{\omega}+\boldsymbol{\nu}_1)} & \overline{\widetilde{m_1}(\boldsymbol{\omega}+\boldsymbol{\nu}_1)} & \overline{\widetilde{m_2}(\boldsymbol{\omega}+\boldsymbol{\nu}_1)} & \overline{\widetilde{m_3}(\boldsymbol{\omega}+\boldsymbol{\nu}_1)} \\
\vdots & \vdots & \vdots & \vdots \\
\overline{\widetilde{m_0}(\boldsymbol{\omega}+\boldsymbol{\nu}_3)} & \overline{\widetilde{m_1}(\boldsymbol{\omega}+\boldsymbol{\pi}_3)} & \overline{\widetilde{m_2}(\boldsymbol{\omega}+\boldsymbol{\nu}_3)} & \overline{\widetilde{m_3}(\boldsymbol{\omega}+\boldsymbol{\nu}_3)}
\end{bmatrix}
\begin{bmatrix}
m_0(\boldsymbol{\omega}) \\
m_1(\boldsymbol{\omega}) \\
m_2(\boldsymbol{\omega}) \\
m_3(\boldsymbol{\omega})
\end{bmatrix}
=
\begin{bmatrix}
1 \\ 0 \\ 0 \\ 0
\end{bmatrix}
\tag{17}
$$

or equivalently $\widetilde{\mathbf{M}}\mathbf{m} = [1,0,0,0]^\top$, where $\widetilde{\mathbf{M}} \in \mathbb{C}^{4\times 4}$ and $\boldsymbol{\nu}_1 = (\pi, 0), \boldsymbol{\nu}_2 = (0,\pi), \boldsymbol{\nu}_3 = (\pi,\pi)$.

Given $\widetilde{m_1}(\boldsymbol{\omega})$, which by symmetry defines $\widetilde{m_2}(\boldsymbol{\omega}), \widetilde{m_3}(\boldsymbol{\omega})$, we can compute m_0,

$$
m_0(\boldsymbol{\omega}) = D^{-1}
\begin{vmatrix}
\widetilde{m_1}(\boldsymbol{\omega}+\boldsymbol{\nu}_1) & \widetilde{m_2}(\boldsymbol{\omega}+\boldsymbol{\nu}_1) & \widetilde{m_3}(\boldsymbol{\omega}+\boldsymbol{\nu}_1) \\
\widetilde{m_1}(\boldsymbol{\omega}+\boldsymbol{\nu}_2) & \widetilde{m_2}(\boldsymbol{\omega}+\boldsymbol{\nu}_2) & \widetilde{m_3}(\boldsymbol{\omega}+\boldsymbol{\nu}_2) \\
\widetilde{m_1}(\boldsymbol{\omega}+\boldsymbol{\nu}_3) & \widetilde{m_2}(\boldsymbol{\omega}+\boldsymbol{\nu}_3) & \widetilde{m_3}(\boldsymbol{\omega}+\boldsymbol{\nu}_3)
\end{vmatrix}
$$

$$
= D^{-1} \det(\widetilde{\mathbf{M}}_{1,1}(\boldsymbol{\omega})), \ D \in \mathbb{R}^+ \tag{18}
$$

if $\widetilde{\mathbf{M}}$ is invertible; both $m_0(\boldsymbol{\omega})$ and $\det(\widetilde{\mathbf{M}}_{1,1}(\boldsymbol{\omega}))$, the minor of $\widetilde{\mathbf{M}}$ associated with $\widetilde{m_0}(\boldsymbol{\omega})$, have invariance by $\frac{2\pi}{3}$.

Remark. For (18) to hold, $m_0(\boldsymbol{\omega})$ and $\det(\widetilde{\mathbf{M}}_{1,1}(\boldsymbol{\omega}))$ having the same phase suffices.

If $\widetilde{m_0}$ is solved, then m_1, m_2 and m_3 are obtained by solving the linear system (17). To get $\widetilde{m_0}(\boldsymbol{\omega})$, we solve

$$
m_0\overline{\widetilde{m_0}}(\boldsymbol{\omega}) + m_0\overline{\widetilde{m_0}}(\boldsymbol{\omega}+\boldsymbol{\nu}_1) + m_0\overline{\widetilde{m_0}}(\boldsymbol{\omega}+\boldsymbol{\nu}_2) + m_0\overline{\widetilde{m_0}}(\boldsymbol{\omega}+\boldsymbol{\nu}_3) = 1 \tag{19}
$$

from expanding $det(\widetilde{\mathbf{M}})$ with respect to the first column. According to Lemma 3.2.1 in [10] based on *Hilbert's Nullstellensatz*, (19) has a solution iff there does not exist $(z_1, z_2) \in (\mathbb{C}^*)^2$, $\mathbb{C}^* = \mathbb{C} \setminus \{0\}$ s.t. $(\pm z_1, \pm z_2)$ are four vanishing points of the z-transform of m_0.

4.1.1   Solving $\widetilde{m_0}(\boldsymbol{\omega})$

In general, there is no efficient algorithm to solve *Hilbert's Nullstellensatz*, and how (16) is solved exactly is not mentioned in [10].

We propose an optimization approach, where (16) is equivalent to a linear constraint and the objective function imposes regularity on $\widetilde{m_0}$. On a $2N \times 2N$ grid $\mathcal{G}$ of $S_0 = [-\pi, \pi) \times [-\pi, \pi)$, s.t. $\forall \boldsymbol{\omega}_j \in \mathcal{G}$, $\boldsymbol{\omega}_j + \boldsymbol{\nu}_1$, $\boldsymbol{\omega}_j + \boldsymbol{\nu}_2$, $\boldsymbol{\omega}_j + \boldsymbol{\nu}_3 \in \mathcal{G}$, (16) is reformulated as

$$
\boldsymbol{A}\,\widetilde{\mathbf{m}}_{\mathbf{0}} = \mathbf{1}_{4N^2}, \tag{20}
$$

$$
\widetilde{\mathbf{m}}_{\mathbf{0}} = [\widetilde{m_0}(\boldsymbol{\omega}_i)]_{i=1,\dots,4N^2} \quad \boldsymbol{A}_{i,j} = m_0(\boldsymbol{\omega}_j)\sum_{k=0}^{3}\delta(\boldsymbol{\omega}_j - \boldsymbol{\omega}_i - \boldsymbol{\nu}_k)
$$

Because the set $\{\boldsymbol{\omega} + \boldsymbol{\nu}_k, k = 0, 1, 2, 3\}$ is invariant under the shift $\boldsymbol{\nu}_i$, $i = 1, 2, 3$, the rows of $\boldsymbol{A}$ corresponding to $\boldsymbol{\omega}$ and $\boldsymbol{\omega} + \boldsymbol{\nu}_i$ are identical and we only need to consider rows corresponds to $\boldsymbol{\omega} \in [-\pi, \pi) \times [-\pi, \pi)/\{\boldsymbol{\nu}_i, i = 0, 1, 2, 3\}$. Therefore, after removing the duplicate rows, $\boldsymbol{A} \in \mathbb{C}^{N^2 \times 4N^2}$ and (20) is under-determinant.
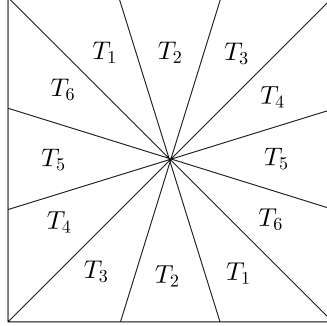
Figure 3: partition of frequency square in six directions, where the essential support of $\widetilde{m_i}(\boldsymbol{\omega})$ is contained in each pair of triangles T_i

We thus use (20) as a linear constraint in quadratic optimization to solve $\widetilde{\mathbf{m_0}}$. Suppose that $\widetilde{m_0}(\boldsymbol{\omega})$ should is smooth, and we build a differential operator $\boldsymbol{D}$ and solve the following minimization problem:

$$\min_{\widetilde{\mathbf{m_0}}} \|\boldsymbol{D}\widetilde{\mathbf{m_0}}\|^2, \quad s.t. \ \boldsymbol{A}\widetilde{\mathbf{m_0}} = \mathbf{1} \tag{21}$$

Or suppose $\widetilde{m_0}(\boldsymbol{\omega})$ decays away from the origin, then we build a diagonal weighting operator $\boldsymbol{W}$, and solve the following minimization problem:

$$\min_{\widetilde{\mathbf{m_0}}} \|\boldsymbol{W}\widetilde{\mathbf{m_0}}\|^2, \quad s.t. \ \boldsymbol{A}\widetilde{\mathbf{m_0}} = \mathbf{1} \tag{22}$$

Supplementary numerical results on solving $\widetilde{m_0}(\boldsymbol{\omega})$ by optimization are provided in Appendix B, where we test this optimization method on pre-designed biorthogonal filters m_0 and $\widetilde{m_0}$.

5   Adaptation to dilated quincunx scheme

Following the same approach, we focus on the design of m_i, $i = 0, \cdots, 6$ and the low pass dual function $\widetilde{m_0}(\boldsymbol{\omega})$, given the high pass directional dual functions $\widetilde{m_i}(\boldsymbol{\omega})$, $i = 1, \cdots, 6$. Assume $\widetilde{m_i}(\boldsymbol{\omega})$, $i = 1, \cdots, 6$ satisfy weak constraints on the direction selectivity of their support.

Definition. The *essential support* Ω_i of a function $\widetilde{m_i}$ is the set $\{\boldsymbol{\omega} : |\widetilde{m_i}(\boldsymbol{\omega})| > |\widetilde{m_j}(\boldsymbol{\omega})|, \ \forall j \neq i\}$.

Let pairs of triangles T_i in Fig.3 contain the essential support of $\widetilde{m_i}$, $i = 1, \cdots, 6$. A minimum symmetry of $\widetilde{m_i}(\boldsymbol{\omega})$ is required such that $\widetilde{m_1}(\boldsymbol{\omega})$ and $\widetilde{m_6}(\boldsymbol{\omega})$ are symmetric with respect to the diagonal, and so are $\widetilde{m_3}(\boldsymbol{\omega})$ and $\widetilde{m_4}(\boldsymbol{\omega})$. (15) takes a similar form to (17), but with $\widetilde{\mathbf{M}} \in \mathbb{C}^{8\times7}$, which is an over-determinant linear system.

9

5.1 Computing m_0

Same as in Section 4.1 , we first compute m_0 and assume that $\widetilde{\mathbf{M}}$ is full rank, otherwise (15) has infinitely many solutions. Moreover, $\widetilde{\mathbf{M}}[2:8,:]$ is singular.

Lemma 5.1. $\widetilde{\mathbf{M}}[2:8,:]$ *is singular* $\forall\boldsymbol{\omega}$.

Proof. If (15) has a solution, then $\forall\boldsymbol{\omega}$, $[1,0,\cdots,0]^\top$ is a linear combination of the columns of $\widetilde{\mathbf{M}}$ and the solution $\mathbf{m}\in Null(\widetilde{\mathbf{M}}[2:8,:])$, hence $\widetilde{\mathbf{M}}[2:8,:]$ being singular is a prerequisite. $\qquad\square$

Therefore, there is a unique row $\widetilde{\mathbf{M}}[k_{\boldsymbol{\omega}},:]$, $k_\omega\in\{2,\cdots,8\}$ such that removing it from $\widetilde{\mathbf{M}}$ gives a non-singular square matrix $\widetilde{\mathbf{M}}[-k_{\boldsymbol{\omega}},:]$. By Cramer's rule,

$$m_0(\boldsymbol{\omega})=det(\widetilde{\mathbf{M}}_{1,1}[-k_{\boldsymbol{\omega}},:])/det(\widetilde{\mathbf{M}}[-k_{\boldsymbol{\omega}},:]),$$

where $det(\widetilde{\mathbf{M}}_{1,1}[-k_{\boldsymbol{\omega}},:])$ is the minor of $\widetilde{\mathbf{M}}[-k_{\boldsymbol{\omega}},:]$ associated with $\widetilde{m_0}(\boldsymbol{\omega})$. Let $C_{\boldsymbol{\omega}}=det(\widetilde{\mathbf{M}}[-k_{\boldsymbol{\omega}},:])$, then we have the following observation.

Lemma 5.2. $C_{\boldsymbol{\omega}}=C_{\boldsymbol{\omega}+\boldsymbol{\pi}_2}=C_{\boldsymbol{\omega}+\boldsymbol{\pi}_4}=C_{\boldsymbol{\omega}+\boldsymbol{\pi}_6}$

Proof Because $\widetilde{M}(\boldsymbol{\omega}+\boldsymbol{\pi}_2)=P_{\boldsymbol{\pi}_2}\widetilde{\mathbf{M}}(\boldsymbol{\omega})$ where $P_{\boldsymbol{\pi}_2}$ is a row permutation matrix, it follows from the definition of $C_{\boldsymbol{\omega}}$ that $C_{\boldsymbol{\omega}}=det\big(\widetilde{\mathbf{M}}[-k_{\boldsymbol{\omega}},:](\boldsymbol{\omega})\big)=det\big(\widetilde{\mathbf{M}}[-k_{\boldsymbol{\omega}+\boldsymbol{\pi}_2},:](\boldsymbol{\omega}+\boldsymbol{\pi}_2)\big)=C_{\boldsymbol{\omega}+\boldsymbol{\pi}_2}$ where $\mathbf{1}_{k_{\boldsymbol{\omega}+\boldsymbol{\pi}_2}}=P_{\boldsymbol{\pi}_2}\mathbf{1}_{k_{\boldsymbol{\omega}}}$. $\qquad\square$

We assume that $m_0\in\mathbb{R}_{\geq0}$ without phase. Let $m_0^C(\boldsymbol{\omega})=m_0(\boldsymbol{\omega})|C_{\boldsymbol{\omega}}|\in\mathbb{R}_{\geq0}$ and $\widetilde{m_0}^C(\boldsymbol{\omega})=\widetilde{m_0}(\boldsymbol{\omega})/|C_{\boldsymbol{\omega}}|$, then Lemma 5.2 implies the following.

Proposition 5.3. $m_0(\boldsymbol{\omega}),\widetilde{m_0}(\boldsymbol{\omega}),m_i(\boldsymbol{\omega})$, $i=1,...,6$ *satisfy* (15) *given* $\widetilde{m_i}(\boldsymbol{\omega})$, $i=1,...,6$ *if and only if* $m_0^C(\boldsymbol{\omega})$, $\widetilde{m_0}^C(\boldsymbol{\omega}),m_i(\boldsymbol{\omega})$, $i=1,...,6$ *do. More generally,* $m_0^C(\boldsymbol{\omega})c(\boldsymbol{\omega}),\widetilde{m_0}^C(\boldsymbol{\omega})c(\boldsymbol{\omega})^{-1},m_i(\boldsymbol{\omega})$, $i=1,...,6$ *satisfy* (15) *if* $c(\boldsymbol{\omega})=c(\boldsymbol{\omega}+\boldsymbol{\pi}_2)=c(\boldsymbol{\omega}+\boldsymbol{\pi}_4)=c(\boldsymbol{\omega}+\boldsymbol{\pi}_6)\neq0$.

According to Proposition 5.3, we can first solve $\widetilde{m_0}^C(\boldsymbol{\omega})$ and $m_0^C(\boldsymbol{\omega})$ and then construct $c(\boldsymbol{\omega})$ for optimal $\widetilde{m_0}(\boldsymbol{\omega})$ and $m_0(\boldsymbol{\omega})$. In particular, m_0^C can be computed without knowing $k_{\boldsymbol{\omega}}$,

$$m_0^C(\boldsymbol{\omega})=m_0(\boldsymbol{\omega})|C_{\boldsymbol{\omega}}|=|det(\widetilde{\mathbf{M}}_{1,1}[-k_{\boldsymbol{\omega}},:])|=\prod_{i=1}^{6}\sigma_i(\widetilde{\mathbf{M}}_{1,1}[-k_{\boldsymbol{\omega}},:])=\prod_{i=1}^{6}\sigma_i(\widetilde{\mathbf{M}}_{1,1}). \tag{23}$$

In practice, we first perform QR decomposition on $\widetilde{\mathbf{M}}^{\square}:=\widetilde{\mathbf{M}}_{1,1}$ and then take the absolute value of the product of the diagonal entries of the upper triangular matrix, $diag(R)$. We propose the following algorithm for bi-orthogonal directional filter construction with dilated quincunx downsampling scheme:

construction of bi-orthogonal basis

Input: $\widetilde{m_i}(\boldsymbol{\omega})$, $i=1,...,6$

1. compute $m_0^C(\boldsymbol{\omega})=\left|det(\widetilde{\mathbf{M}}_{1,1}[-k_{\boldsymbol{\omega}},:])\right|$

2. compute $\widetilde{m_0}^C(\boldsymbol{\omega})$, such that (15) is solvable and (16) holds

3. solve $m_i(\boldsymbol{\omega})$, $i = 1, ..., 6$ according to (15)

4. design $c(\boldsymbol{\omega})$ and let $m_0(\boldsymbol{\omega}) = m_0^C(\boldsymbol{\omega})c(\boldsymbol{\omega})$, $\widetilde{m_0}(\boldsymbol{\omega}) = \widetilde{m_0}^C(\boldsymbol{\omega})\bar{c}(\boldsymbol{\omega})^{-1}$

5.2 Singularity condition on $\widetilde{\mathbf{M}}[2:8,:]$ and discontinuity of $\widetilde{m_i}(\boldsymbol{\omega})$

Lemma 5.1 is equivalent to the following singularity constraint,

$$0 = \det(\widetilde{\mathbf{M}}[2:8,:]) = \widetilde{m_0}(\boldsymbol{\omega} + \boldsymbol{\pi}_2)\det(\widetilde{\mathbf{M}}^\square[-2,:]) + \widetilde{m_0}(\boldsymbol{\omega} + \boldsymbol{\pi}_4)\det(\widetilde{\mathbf{M}}^\square[-4,:])$$
$$+ \widetilde{m_0}(\boldsymbol{\omega} + \boldsymbol{\pi}_6)\det(\widetilde{\mathbf{M}}^\square[-6,:]).$$

Let $\widetilde{\mathbf{m}}^i(\boldsymbol{\omega}) = [\widetilde{m_1}(\boldsymbol{\omega} + \boldsymbol{\pi}_i) \cdots, \widetilde{m_6}(\boldsymbol{\omega} + \boldsymbol{\pi}_i)] \in \mathbb{C}^6$, $i = 0, \cdots, 7$, and define
$d_{i,j}(\boldsymbol{\omega}) = \det([\widetilde{\mathbf{m}}^{k_1}(\boldsymbol{\omega})^\top, \cdots, \widetilde{\mathbf{m}}^{k_6}(\boldsymbol{\omega})^\top])$, $0 \leq k_1 < \cdots < k_l < \cdots < k_6 \leq 7, k_l \neq i, j$,
then the above singularity condition on $\widetilde{\mathbf{M}}[2:8,:]$ at $\boldsymbol{\omega}$ can be rewritten as follows,

$$[0, d_{0,2}(\boldsymbol{\omega}), d_{0,4}(\boldsymbol{\omega}), d_{0,6}(\boldsymbol{\omega})][\widetilde{m_0}(\boldsymbol{\omega}), \widetilde{m_0}(\boldsymbol{\omega} + \boldsymbol{\pi}_2), \widetilde{m_0}(\boldsymbol{\omega} + \boldsymbol{\pi}_4), \widetilde{m_0}(\boldsymbol{\omega} + \boldsymbol{\pi}_6)]^\top = 0$$

It is easy to verify that the above singular condition at $\boldsymbol{\omega} + \boldsymbol{\pi}_2$ is equivalent to

$$[-d_{0,2}(\boldsymbol{\omega}), 0, d_{2,4}(\boldsymbol{\omega}), d_{2,6}][\widetilde{m_0}(\boldsymbol{\omega}), \widetilde{m_0}(\boldsymbol{\omega} + \boldsymbol{\pi}_2), \widetilde{m_0}(\boldsymbol{\omega} + \boldsymbol{\pi}_4), \widetilde{m_0}(\boldsymbol{\omega} + \boldsymbol{\pi}_6)]^\top = 0$$

Similarly, rewrite the singularity condition at $\boldsymbol{\omega} + \boldsymbol{\pi}_4$ and $\boldsymbol{\omega} + \boldsymbol{\pi}_6$ in the coordinate of $\boldsymbol{\omega}$ and combine all four conditions, we have the following linear constraint

$$\mathfrak{D}(\boldsymbol{\omega})\begin{bmatrix} \widetilde{m_0}(\boldsymbol{\omega}) \\ \widetilde{m_0}(\boldsymbol{\omega} + \boldsymbol{\pi}_2) \\ \widetilde{m_0}(\boldsymbol{\omega} + \boldsymbol{\pi}_4) \\ \widetilde{m_0}(\boldsymbol{\omega} + \boldsymbol{\pi}_6) \end{bmatrix} = \begin{bmatrix} 0 & d_{0,2} & d_{0,4} & d_{0,6} \\ -d_{0,2} & 0 & d_{2,4} & d_{2,6} \\ -d_{0,4} & -d_{2,4} & 0 & d_{4,6} \\ -d_{0,6} & -d_{2,6} & -d_{4,6} & 0 \end{bmatrix}\begin{bmatrix} \widetilde{m_0}(\boldsymbol{\omega}) \\ \widetilde{m_0}(\boldsymbol{\omega} + \boldsymbol{\pi}_2) \\ \widetilde{m_0}(\boldsymbol{\omega} + \boldsymbol{\pi}_4) \\ \widetilde{m_0}(\boldsymbol{\omega} + \boldsymbol{\pi}_6) \end{bmatrix} = \begin{bmatrix} 0 \\ 0 \\ 0 \\ 0 \end{bmatrix},$$
$$(24)$$

where $\mathfrak{D}(\boldsymbol{\omega})$ is anti-symmetric. Because $\mathfrak{D}(\boldsymbol{\omega})$ is independent of $m_0(\boldsymbol{\omega})$, (24) holds for $\widetilde{m_0}^C(\boldsymbol{\omega})$ as well.

On the other hand, given $m_0(m_0^C)$, $\widetilde{m_0}(\widetilde{m_0}^C)$ has to satisfy the identity constraint (16). (16) and (24) together imply the following proposition,

Proposition 5.4. *Given $\widetilde{m_i}, i = 1, \cdots, 6$, (15) has no solution for any $\widetilde{m_0}$, if $\exists \boldsymbol{\omega}, s.t.[m_0(\boldsymbol{\omega}), m_0(\boldsymbol{\omega} + \pi_2), m_0(\boldsymbol{\omega} + \pi_4), m_0(\boldsymbol{\omega} + \pi_6)]$ is a linear combination of the rows of $\mathfrak{D}(\omega)$.*

Proposition 5.4 provides a necessary condition such that the numerical optimization solving $\widetilde{m_0}$ is feasible.

Definition Let the cone $T_i = T_i^- \bigcup T_i^+$, where T_i^-, T_i^+ are halves of T_i adjacent to T_{i-1} and T_{i+1} respectively. $\widetilde{m_i}$ *concentrates* within cone T_i if supp$(\widetilde{m_i}) \subset T_{i-1}^+ \bigcup T_i \bigcup T_{i+1}^-$ and $\int_\Omega |\widetilde{m_i}| > \int_{\Omega'} |\widetilde{m_i}|, \forall \Omega \subset T_i \bigcap \text{supp}(\widetilde{m_i}), |\Omega| > 0$, where Ω' is symmetric to Ω with respect to the boundary of T_i.

Given directional selective $\widetilde{m_i}(\boldsymbol{\omega})$ that concentrates in T_i, we study the feasibility condition in Proposition 5.4 specifically on the domain $S_\rho = \{(\omega_x, \omega_y)| \|\omega\| <$
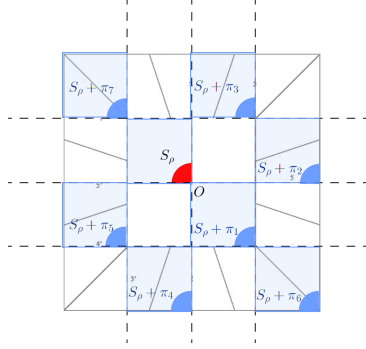
Figure 4: S_ρ and its shifts

$\rho, \omega_x < 0, \omega_y < 0\}$. When ρ is small enough, $\widetilde{m_i}(\boldsymbol{\omega})$ is zero on all but a few sets $S_\rho + \boldsymbol{\pi}_j$ (see Fig.4 for reference of S_ρ and its shifts), thus $\widetilde{\mathbf{m}}^i(\boldsymbol{\omega})$ is sparse on S_ρ in the following form

$$\begin{bmatrix} \widetilde{\mathbf{m}}^0 \\ \widetilde{\mathbf{m}}^2 \\ \widetilde{\mathbf{m}}^4 \\ \widetilde{\mathbf{m}}^6 \\ \widetilde{\mathbf{m}}^1 \\ \widetilde{\mathbf{m}}^3 \\ \widetilde{\mathbf{m}}^5 \\ \widetilde{\mathbf{m}}^7 \end{bmatrix} = \begin{bmatrix} 0 & 0 & 0 & 0 & 0 & 0 \\ 0 & * & * & 0 & 0 & 0 \\ 0 & 0 & 0 & * & * & 0 \\ * & 0 & 0 & 0 & 0 & * \\ * & 0 & 0 & 0 & 0 & * \\ 0 & 0 & * & * & 0 & 0 \\ 0 & 0 & * & * & 0 & 0 \\ * & 0 & 0 & 0 & 0 & * \end{bmatrix} = \boldsymbol{P}\,\widetilde{\mathbf{M}}[:, 2:7], \qquad (25)$$

where $\boldsymbol{P}$ is a row permutation matrix.

Lemma 5.5. $rank(\widetilde{\mathbf{m}}^1, \widetilde{\mathbf{m}}^7) = 1$ in (25).

Proof. We make the following observation of $\widetilde{\mathbf{m}}^i$ in (25):

(i) $\widetilde{\mathbf{m}}^0$ is a zero vector

(ii) $\widetilde{\mathbf{m}}^2$ and $\widetilde{\mathbf{m}}^4$ are linearly independent of each other and the rest of $\widetilde{\mathbf{m}}^i$

(iii) $span\{\widetilde{\mathbf{m}}^1, \widetilde{\mathbf{m}}^6, \widetilde{\mathbf{m}}^7\} \perp span\{\widetilde{\mathbf{m}}^3, \widetilde{\mathbf{m}}^5\}$ and $rank(\widetilde{\mathbf{m}}^1, \widetilde{\mathbf{m}}^6, \widetilde{\mathbf{m}}^7) \leq 2$, $rank(\widetilde{\mathbf{m}}^3, \widetilde{\mathbf{m}}^5) \leq 2$

Because $\widetilde{\mathbf{M}}[2:8, 2:7]$ consists of rows $\widetilde{\mathbf{m}}^i$, $i \neq 0$, and the low-pass function $m_0(\boldsymbol{\omega}) \neq 0, \forall \boldsymbol{\omega} \in S_\rho$, or equivalently $rank(\widetilde{\mathbf{M}}[2:8, 2:7](\boldsymbol{\omega})) = 6$, it follows from (ii) and (iii) that $rank(\widetilde{\mathbf{m}}^1, \widetilde{\mathbf{m}}^6, \widetilde{\mathbf{m}}^7) = 2$ and $rank(\widetilde{\mathbf{m}}^3, \widetilde{\mathbf{m}}^5) = 2$.
On the other hand, (ii) implies that

$$rank(\widetilde{\mathbf{M}}[2:8, 2:7](\boldsymbol{\omega} + \boldsymbol{\pi}_2)) = rank(\widetilde{\mathbf{m}}^4, \widetilde{\mathbf{m}}^6, \widetilde{\mathbf{m}}^1, \widetilde{\mathbf{m}}^3, \widetilde{\mathbf{m}}^5, \widetilde{\mathbf{m}}^7) \leq 5$$

and $rank(\widetilde{\mathbf{M}}[2:8, 2:7](\boldsymbol{\omega} + \boldsymbol{\pi}_4)) = rank(\widetilde{\mathbf{m}}^2, \widetilde{\mathbf{m}}^6, \widetilde{\mathbf{m}}^1, \widetilde{\mathbf{m}}^3, \widetilde{\mathbf{m}}^5, \widetilde{\mathbf{m}}^7) \leq 5$ likewise. Therefore, $m_0(\boldsymbol{\omega} + \boldsymbol{\pi}_2) = m_0(\boldsymbol{\omega} + \boldsymbol{\pi}_4) = 0$.
If $\widetilde{\mathbf{m}}^1$ and $\widetilde{\mathbf{m}}^7$ are linearly independent, then $rank(\widetilde{\mathbf{m}}^2, \widetilde{\mathbf{m}}^4, \widetilde{\mathbf{m}}^1, \widetilde{\mathbf{m}}^3, \widetilde{\mathbf{m}}^5, \widetilde{\mathbf{m}}^7) = 6$ and $m_0^C(\boldsymbol{\omega} + \boldsymbol{\pi}_6) \neq 0$, hence $m_0(\boldsymbol{\omega} + \boldsymbol{\pi}_6) \neq 0$. Therefore, $[m_0(\boldsymbol{\omega}), m_0(\boldsymbol{\omega} +$

12

$\boldsymbol{\pi}_2), m_0(\boldsymbol{\omega} + \boldsymbol{\pi}_4), m_0(\boldsymbol{\omega} + \boldsymbol{\pi}_6)] = [m_0(\boldsymbol{\omega}), 0, 0, m_0(\boldsymbol{\omega} + \boldsymbol{\pi}_6)]$. In addition, $d_{i,j} = 0, \forall (i,j)$ except $(0,6)$, so $\mathfrak{D}(\boldsymbol{\omega}) = [d_{0,6}, 0, 0, 0]^\top [0, 0, 0, 1] + [0, 0, 0, d_{0,6}]^\top [-1, 0, 0, 0]$. By Prop.5.4, the linear system (15) has no solution $\forall \widetilde{m_0}$ and the lemma is proofed. $\square$

Lemma 5.6. *If* $\widetilde{m_1}(\boldsymbol{\omega})(\widetilde{m_6}(\boldsymbol{\omega}))$ *concentrates in* $T_1(T_6)$ *and its essential support* $\Omega_1 \subset T_1(\Omega_6 \subset T_6)$, *then* $|\widetilde{m_6}(\boldsymbol{\omega})| > |\widetilde{m_1}(\boldsymbol{\omega})|$ *a.e. on* $T_6 \bigcap supp(\widetilde{m_6})$ $(|\widetilde{m_1}(\boldsymbol{\omega})| > |\widetilde{m_6}(\boldsymbol{\omega})|$ *a.e. on* $T_1 \bigcap supp(\widetilde{m_1})$*).*

Proof Let $B_6 = \{\boldsymbol{\omega} : |\widetilde{m_6}(\boldsymbol{\omega})| \leq |\widetilde{m_1}(\boldsymbol{\omega})|, \widetilde{m_1}(\boldsymbol{\omega}) \neq 0\} \bigcap T_6$ and B_1 be its mirror set with respect to $\omega_y = \omega_x$ and suppose $|B_6| > 0$, then $\int_{B_6} |\widetilde{m_6}(\boldsymbol{\omega})| \leq \int_{B_6} |\widetilde{m_1}(\boldsymbol{\omega})|$. Since $\widetilde{m_1}(\boldsymbol{\omega})$ concentrates in T_1, we know $\int_{B_1} |\widetilde{m_1}(\boldsymbol{\omega})| > \int_{B_6} |\widetilde{m_1}(\boldsymbol{\omega})|$. On the other hand, due to the symmetry of $\widetilde{m_1}(\boldsymbol{\omega}), \widetilde{m_6}(\boldsymbol{\omega})$ and B_1, B_6, $\int_{B_1} |\widetilde{m_1}(\boldsymbol{\omega})| = \int_{B_6} |\widetilde{m_6}(\boldsymbol{\omega})|$, hence $\int_{B_6} |\widetilde{m_1}(\boldsymbol{\omega})| \geq \int_{B_1} |\widetilde{m_1}(\boldsymbol{\omega})|$ which results in contradiction. $\square$

Proposition 5.7. *If* $m_1 (m_6)$ *concentrates within* $T_1 (T_6)$ *and* $\Omega_1 \subset T_1 (\Omega_6 \subset T_6)$, *then* $\widetilde{m_1}(\boldsymbol{\omega}) = \widetilde{m_6}(\boldsymbol{\omega}) = 0$, *a.e.* $\boldsymbol{\omega} \in S_\rho + \boldsymbol{\pi}_1$.

Proof. By Lemma 5.6, $|\widetilde{m_1}(\boldsymbol{\omega})| > |\widetilde{m_6}(\boldsymbol{\omega})|$ *a.e.* on $\Omega'_1 := (S_\rho + \boldsymbol{\pi}_7) \bigcap T_1 = (S_\rho + \boldsymbol{\pi}_1) \bigcap T_6 + (\pi, \pi)$. By Lemma 5.5, $\exists \alpha_{\boldsymbol{\omega}} \in \mathbb{C}, s.t. \widetilde{\mathbf{m}}^1(\boldsymbol{\omega}) = \alpha_{\boldsymbol{\omega}} \widetilde{\mathbf{m}}^7(\boldsymbol{\omega})$, hence $|\widetilde{m_1}(\boldsymbol{\omega})| = |\alpha_{\boldsymbol{\omega}}| \cdot |\widetilde{m_1}(\boldsymbol{\omega} - (\pi, \pi))| \geq |\alpha_{\boldsymbol{\omega}}| \cdot |\widetilde{m_6}(\boldsymbol{\omega} - (\pi, \pi))| = |\widetilde{m_6}(\boldsymbol{\omega})|, a.e.$ on $\Omega'_6 := (S_\rho + \pi_1) \bigcap T_6$. Therefore, $\int_{\Omega'_6} |\widetilde{m_1}| \geq \int_{\Omega'_6} |\widetilde{m_6}|$, which will contradict Lemma 5.6 unless $|\Omega'_6 \bigcap supp(\widetilde{m_6})| = 0$, or equivalently $\alpha_{\boldsymbol{\omega}} = 0$ and so $\widetilde{m_6}(\boldsymbol{\omega}) = \widetilde{m_1}(\boldsymbol{\omega}) = 0$, *a.e.* on $(S_\rho + \boldsymbol{\pi}_1) \bigcap T_6$. By symmetry, $\widetilde{m_6}(\boldsymbol{\omega}) = \widetilde{m_1}(\boldsymbol{\omega}) = 0$, *a.e.* on $(S_\rho + \boldsymbol{\pi}_1) \bigcap T_1$ as well. $\square$

Proposition 5.8. $\widetilde{m_1}(\boldsymbol{\omega}), \widetilde{m_3}(\boldsymbol{\omega})$ *are not continuous at* $\boldsymbol{\pi}_1, \boldsymbol{\pi}_7$ *and* $\widetilde{m_5}(\boldsymbol{\omega}), \widetilde{m_7}(\boldsymbol{\omega})$ *are not continuous at* $\boldsymbol{\pi}_3, \boldsymbol{\pi}_5$.

Proof If $\widetilde{m_1}(\boldsymbol{\omega})$ is continuous at $\boldsymbol{\pi}_1$, then $\widetilde{m_1}(\boldsymbol{\pi}_1) = \lim_{\alpha \to 1^-} \widetilde{m_1}(\boldsymbol{\omega}(\alpha)) = 0$, where $\{\boldsymbol{\omega}(\alpha), 0 \leq \alpha < 1\} \subset S_\rho + \boldsymbol{\pi}_1$ and $\boldsymbol{\omega}(1^-) = \boldsymbol{\pi}_1$. Similarly, we have $\widetilde{m_6}(\boldsymbol{\pi}_1) = 0$. Applying the same argument of S_ρ to its rotation of 180 degree, we have $\widetilde{m_1}(\boldsymbol{\pi}_7) = \widetilde{m_6}(\boldsymbol{\pi}_7) = 0$. Therefore $\widetilde{\mathbf{m}}^1(0) = \widetilde{\mathbf{m}}^7(0) = \mathbf{0}$ and from (23) $m_0^C(0) = 0$ so that $m_0(0) = 0$, which results in contradiction. $\square$

The following theorem summarizes the necessary condition derived from the singularity condition of $\widetilde{\mathbf{M}}[2:8,:](24)$.

Theorem 5.9. *If* $\widetilde{m_i}(\boldsymbol{\omega})$ *concentrates in* T_i *with essential support* $\Omega_i \subset T_i$ *and* m_1, m_6 *are symmetric to each other or* m_3, m_4 *are symmetric to each other, then* (15) *doesn't have feasible solution given continuous* $\widetilde{m_i}(\boldsymbol{\omega})$.

5.3 Design of input $\widetilde{m_i}(\boldsymbol{\omega})$

Following the orthonormal construction in [9], we consider $\widetilde{m_1}(\boldsymbol{\omega}), \cdots, \widetilde{m_6}(\boldsymbol{\omega})$ in the form

$$\widetilde{m_k}(\boldsymbol{\omega}) = e^{-i\eta_k^\top \omega} |\widetilde{m_k}(\boldsymbol{\omega})|, \tag{26}$$

and $|\widetilde{m_k}(\boldsymbol{\omega})|$ have certain symmetry. We want to design the phase $\boldsymbol{\eta}_k$ such that $m_0(\boldsymbol{\omega}) > 0$, $\forall \omega \in S_1$. This is the same as requiring $\widetilde{\mathbf{M}}^\square$ to be full rank. We first show the necessary conditions on phases $\boldsymbol{\eta}$ of the full rank requirement on $\widetilde{\mathbf{M}}^\square$.

Lemma 5.10. *If* $\exists \boldsymbol{\omega} \in D_1 := \{\omega_x = \omega_y, \omega_x \in (-\frac{\pi}{2}, 0)\}$, *s.t.* $m_0(\boldsymbol{\omega}) > 0$, *then* $(\boldsymbol{\eta}_1 - \boldsymbol{\eta}_6)^\top (\boldsymbol{\pi}_6 - \boldsymbol{\pi}_7) \neq 0 (mod\, 2\pi)$.

Proof If $m_0(\boldsymbol{\omega}) > 0$, $\boldsymbol{\omega} \in D_1$ then $\widetilde{\mathbf{M}}^\square$ is full rank, hence its columns are linearly independent. Due to symmetry, $|\widetilde{m_1}(\boldsymbol{\omega})| = |\widetilde{m_6}(\boldsymbol{\omega})|$ on $\{\omega_x = \omega_y\}$. Let $A = |\widetilde{m_1}(\boldsymbol{\omega} + \boldsymbol{\pi}_1)| = |\widetilde{m_6}(\boldsymbol{\omega} + \boldsymbol{\pi}_1)|$ and $B = |\widetilde{m_1}(\boldsymbol{\omega} + \boldsymbol{\pi}_6)| = |\widetilde{m_6}(\boldsymbol{\omega} + \boldsymbol{\pi}_6)|$, then the first and the last columns of $\widetilde{\mathbf{M}}^\square$ are

$$\widetilde{\mathbf{M}}^\square[:, 1] = \begin{bmatrix} 0 \\ \vdots \\ 0 \\ A e^{i \boldsymbol{\eta}_1^\top (\boldsymbol{\omega} + \boldsymbol{\pi}_6)} \\ B e^{i \boldsymbol{\eta}_1^\top (\boldsymbol{\omega} + \boldsymbol{\pi}_7)} \end{bmatrix} \quad \text{and} \quad \widetilde{\mathbf{M}}^\square[:, 6] = \begin{bmatrix} 0 \\ \vdots \\ 0 \\ A e^{i \boldsymbol{\eta}_6^\top (\boldsymbol{\omega} + \boldsymbol{\pi}_6)} \\ B e^{i \boldsymbol{\eta}_6^\top (\boldsymbol{\omega} + \boldsymbol{\pi}_7)} \end{bmatrix}.$$

Therefore, $\widetilde{\mathbf{M}}^\square[:, 1]$ and $\widetilde{\mathbf{M}}^\square[:, 6]$ are linearly independent implies that $e^{i(\boldsymbol{\eta}_1 - \boldsymbol{\eta}_6)^\top (\boldsymbol{\omega} + \boldsymbol{\pi}_6)} \neq e^{i(\boldsymbol{\eta}_1 - \boldsymbol{\eta}_6)^\top (\boldsymbol{\omega} + \boldsymbol{\pi}_7)}$ or equivalently $(\boldsymbol{\eta}_1 - \boldsymbol{\eta}_6)^\top (\boldsymbol{\pi}_6 - \boldsymbol{\pi}_7) \neq 0 (\text{mod} 2\pi)$. $\square$

Similarly, if $\exists \boldsymbol{\omega} \in \{\omega_y = \omega_x, \omega_x \in (0, \frac{\pi}{2})\}$, s.t. $m_0(\boldsymbol{\omega}) > 0$, then $(\boldsymbol{\eta}_1 - \boldsymbol{\eta}_6)^\top (\boldsymbol{\pi}_6 - \boldsymbol{\pi}_1) \neq 0 (\text{mod}\, 2\pi)$. These two conditions are equivalent to

$$(\boldsymbol{\eta}_1 - \boldsymbol{\eta}_6)^\top (\pi/2, \pi/2) \neq 0 (\text{mod}\, 2\pi) \tag{c1.1}$$

given that $\boldsymbol{\eta}_1$ and $\boldsymbol{\eta}_6$ are integer phases. A stronger condition is to require $\widetilde{\mathbf{M}}^\square[:, 1]$ and $\widetilde{\mathbf{M}}^\square[:, 6]$ be orthogonal, which is equivalent to

$$(\boldsymbol{\eta}_1 - \boldsymbol{\eta}_6)^\top (\pi/2, \pi/2) = \pi\, (\text{mod}\, 2\pi). \tag{c2.1}$$

Considering the other diagonal segment $\{\omega_y = -\omega_x, |\omega_x| < \frac{\pi}{2}\}$, we have

$$(\boldsymbol{\eta}_3 - \boldsymbol{\eta}_4)^\top (-\pi/2, \pi/2) \neq 0 (\text{mod}\, 2\pi) \tag{c1.2}$$

from the full rank condition and

$$(\boldsymbol{\eta}_3 - \boldsymbol{\eta}_4)^\top (-\pi/2, \pi/2) = \pi (\text{mod}, 2\pi) \tag{c2.2}$$

from the stronger orthogonal condition. *Remark* If $|\widetilde{m_1}(\boldsymbol{\omega})| = |\widetilde{m_2}(\boldsymbol{\omega})|$ on $\{\omega_y = 3\omega_x, |\omega_x| > \frac{\pi}{2}\}$ and $m_0(\boldsymbol{\omega}) > 0$ on $\{\omega_y = 3\omega_x \pm \pi, |\omega_y| < \frac{\pi}{2}\}$, then the same conditions (**c1**) and (**c2**) can be derived from full rank and orthogonal conditions respectively for tuples $(\boldsymbol{\eta}_1, \boldsymbol{\eta}_2, (-\pi/2, \pi/2))$, $(\boldsymbol{\eta}_2, \boldsymbol{\eta}_3, (\pi/2, \pi/2))$, $(\boldsymbol{\eta}_4, \boldsymbol{\eta}_5, (\pi/2, \pi/2))$ and $(\boldsymbol{\eta}_5, \boldsymbol{\eta}_6, (-\pi/2, \pi/2))$.

Next, we investigate $\widetilde{\mathbf{M}}^\square$ at the origin, where the two diagonals meet.

Proposition 5.11. *If* $m_0(0) > 0$, *then* $\boldsymbol{\pi}_1^\top (\boldsymbol{\eta}_1 - \boldsymbol{\eta}_6) \neq \pi (mod\, 2\pi)$ *or* $\boldsymbol{\pi}_3^\top (\boldsymbol{\eta}_3 - \boldsymbol{\eta}_4) \neq \pi (mod\, 2\pi)$.

Proof $\widetilde{\mathbf{M}}^{\square}(0)$ takes the following form

$$\begin{bmatrix} * & 0 & 0 & 0 & 0 & * \\ 0 & * & 0 & 0 & 0 & 0 \\ 0 & 0 & * & * & 0 & 0 \\ 0 & 0 & 0 & 0 & * & 0 \\ 0 & 0 & * & * & 0 & 0 \\ * & 0 & * & * & 0 & * \\ * & 0 & 0 & 0 & 0 & * \end{bmatrix}$$

The second and the fifth columns of $\widetilde{\mathbf{M}}^{\square}$ have single non-zero entry, $\widetilde{m}_2(\boldsymbol{\pi}_2)$ and $\widetilde{m}_5(\boldsymbol{\pi}_4)$ respectively, and are orthogonal to all the rest columns, hence the full-rank constraint of $\widetilde{\mathbf{M}}^{\square}$ is reduced to the full-rank constraint on its sub-matrix (with permutation of rows and columns)

$$\overline{\mathrm{B}} := \overline{\widetilde{\mathbf{M}}^{\square}}[-2, -4, :] = \begin{bmatrix} \widetilde{m}_1(\boldsymbol{\pi}_6) & \widetilde{m}_6(\boldsymbol{\pi}_6) & \widetilde{m}_3(\boldsymbol{\pi}_6) & \widetilde{m}_4(\boldsymbol{\pi}_6) \\ \widetilde{m}_1(\boldsymbol{\pi}_1) & \widetilde{m}_6(\boldsymbol{\pi}_1) & 0 & 0 \\ \widetilde{m}_1(\boldsymbol{\pi}_7) & \widetilde{m}_6(\boldsymbol{\pi}_7) & 0 & 0 \\ 0 & 0 & \widetilde{m}_3(\boldsymbol{\pi}_3) & \widetilde{m}_4(\boldsymbol{\pi}_3) \\ 0 & 0 & \widetilde{m}_3(\boldsymbol{\pi}_5) & \widetilde{m}_4(\boldsymbol{\pi}_5) \end{bmatrix}$$

Without loss of generality, let $|\widetilde{m}_1(\boldsymbol{\pi}_1)| = |\widetilde{m}_1(\boldsymbol{\pi}_7)| = |\widetilde{m}_6(\boldsymbol{\pi}_1)| = |\widetilde{m}_6(\boldsymbol{\pi}_7)| = |\widetilde{m}_3(\boldsymbol{\pi}_3)| = |\widetilde{m}_3(\boldsymbol{\pi}_5)| = |\widetilde{m}_4(\boldsymbol{\pi}_3)| = |\widetilde{m}_4(\boldsymbol{\pi}_5)| = a$ and $|\widetilde{m}_1(\boldsymbol{\pi}_6)| = |\widetilde{m}_6(\boldsymbol{\pi}_6)| = |\widetilde{m}_3(\boldsymbol{\pi}_6)| = |\widetilde{m}_4(\boldsymbol{\pi}_6)| = b$. Rewrite $\overline{\mathrm{B}}$ as follows,

$$\overline{\mathrm{B}} = \begin{bmatrix} be^{-i\boldsymbol{\pi}_6^\top \boldsymbol{\eta}_1} & be^{-i\boldsymbol{\pi}_6^\top \boldsymbol{\eta}_6} & be^{-i\boldsymbol{\pi}_6^\top \boldsymbol{\eta}_3} & be^{-i\boldsymbol{\pi}_6^\top \boldsymbol{\eta}_4} \\ ae^{-i\boldsymbol{\pi}_1^\top \boldsymbol{\eta}_1} & ae^{-i\boldsymbol{\pi}_1^\top \boldsymbol{\eta}_6} & 0 & 0 \\ ae^{i\boldsymbol{\pi}_1^\top \boldsymbol{\eta}_1} & ae^{i\boldsymbol{\pi}_1^\top \boldsymbol{\eta}_6} & 0 & 0 \\ 0 & 0 & ae^{-i\boldsymbol{\pi}_3^\top \boldsymbol{\eta}_3} & ae^{-i\boldsymbol{\pi}_3^\top \boldsymbol{\eta}_4} \\ 0 & 0 & ae^{i\boldsymbol{\pi}_3^\top \boldsymbol{\eta}_3} & ae^{i\boldsymbol{\pi}_3^\top \boldsymbol{\eta}_4} \end{bmatrix}$$

The product of singular values of $\boldsymbol{B}$ is

$$\sqrt{\det(\boldsymbol{B}^* \boldsymbol{B})} = 4a^3 \sqrt{a^2 K_1^2 K_2^2 + b^2(Q_1 K_2^2 + Q_2 K_1^2)}, \tag{27}$$

where $Q_1 = 1 - \cos(\boldsymbol{\pi}_6^\top(\boldsymbol{\eta}_1 - \boldsymbol{\eta}_6)) \cos(\boldsymbol{\pi}_1^\top(\boldsymbol{\eta}_1 - \boldsymbol{\eta}_6)), Q_2 = 1 - \cos(\boldsymbol{\pi}_6^\top(\boldsymbol{\eta}_3 - \boldsymbol{\eta}_4)) \cos(\boldsymbol{\pi}_3^\top(\boldsymbol{\eta}_3 - \boldsymbol{\eta}_4)), K_1 = \sin(\boldsymbol{\pi}_1^\top(\boldsymbol{\eta}_1 - \boldsymbol{\eta}_6)), K_2 = \sin(\boldsymbol{\pi}_3^\top(\boldsymbol{\eta}_3 - \boldsymbol{\eta}_4))$.

If the previous strong orthogonal condition on $\boldsymbol{\eta}_1, \boldsymbol{\eta}_3, \boldsymbol{\eta}_4, \boldsymbol{\eta}_6$ holds, then $K_1 = K_2 = 0$ and $m_0(0) = m_0^C(0) = 0$. Therefore, the strong orthogonal condition (**c2**) cannot be satisfied at the same time. In particular, we consider the following constraints on phase $\boldsymbol{\eta}_k \in \mathbb{Z}^2$, $k = 1, \cdots, 6$:

$(\boldsymbol{\eta}_1 - \boldsymbol{\eta}_2)^\top(-\pi/2, \pi/2) = (\boldsymbol{\eta}_5 - \boldsymbol{\eta}_6)^\top(-\pi/2, \pi/2) = \pi \,(\mathrm{mod}\, 2\pi)$

$(\boldsymbol{\eta}_2 - \boldsymbol{\eta}_3)^\top(\pi/2, \pi/2) = (\boldsymbol{\eta}_4 - \boldsymbol{\eta}_5)^\top(\pi/2, \pi/2) = \pi \,(\mathrm{mod}\, 2\pi) \tag{28}$

$(\boldsymbol{\eta}_3 - \boldsymbol{\eta}_4)^\top(-\pi/2, \pi/2) = -\pi/2 \,(\mathrm{mod}\, 2\pi) \quad (\boldsymbol{\eta}_6 - \boldsymbol{\eta}_1)^\top(\pi/2, \pi/2) = \pi/2 \,(\mathrm{mod}\, 2\pi)$

where we require strong orthogonal constraints on pair of shifts corresponding to $\widetilde{m}$ function with non-diagonal common boundary and weaker constraints on

$(\boldsymbol{\eta}_1, \boldsymbol{\eta}_6)$ and $(\boldsymbol{\eta}_3, \boldsymbol{\eta}_4)$. A solution to (28) is

$$\boldsymbol{\eta}_1 = (0,0), \ \boldsymbol{\eta}_2 = (-1,1), \ \boldsymbol{\eta}_3 = (0,2),$$
$$\boldsymbol{\eta}_4 = (1,0), \ \boldsymbol{\eta}_5 = (0,-1), \ \boldsymbol{\eta}_6 = (0,1). \quad (29)$$

5.4   solving m_i

In the final step, we substitute $\widetilde{m_0}^C(\boldsymbol{\omega})$ and $m_0^C(\boldsymbol{\omega})$ into (15) and rewrite it into the following linear system,

$$\overline{\overline{\mathbf{M}}}[:, 2:7]\,\mathbf{m}[2:7](\boldsymbol{\omega}) = \begin{bmatrix} 1 - m_0^C \overline{\widetilde{m_0}^C}(\boldsymbol{\omega}) \\ 0 \\ -m_0^C \overline{\widetilde{m_0}^C}(\boldsymbol{\omega} + \boldsymbol{\pi}_2) \\ \vdots \\ 0 \end{bmatrix} =: \mathbf{b}(\boldsymbol{\omega}). \quad (30)$$

The solution of (30) depends only on $m_0^C \overline{\widetilde{m_0}^C}$, or equivalently $m_0 \overline{\widetilde{m_0}}$.

6   Numerical Experiments

6.1   solving m_0^C

A set of $\widetilde{m_i}(\boldsymbol{\omega})$ that satisfy the conditions of Theorem 5.9 with phase terms in (29) is used as the input of (15). The left figure in Fig.5 shows the absolute value of $\widetilde{m_i}(\boldsymbol{\omega})$. In particular, $\widetilde{m_i}(\boldsymbol{\omega}) = 0, \forall \omega \in S_1$. We follow the construction process in Section 5.1 and obtain m_0^C shown in the right of Fig.5, in both normal scale and log scale. We perform a numerical sanity check on the necessary condition in Proposition 5.4, that is $\forall \boldsymbol{\omega}, \ s.t.[m_0(\boldsymbol{\omega}), m_0(\boldsymbol{\omega} + \boldsymbol{\pi}_2), m_0(\boldsymbol{\omega} + \boldsymbol{\pi}_4), m_0(\boldsymbol{\omega} + \boldsymbol{\pi}_6)]$ is not a linear combination of the rows of $\mathfrak{D}(\boldsymbol{\omega})$ in (24). Equivalently, we compute the following quantity

$$\vartheta = 1 - \|V^\top \mathfrak{m}_0\| / \|\mathfrak{m}_0\|,$$

where $\mathfrak{m}_0(\boldsymbol{\omega}) = [m_0(\boldsymbol{\omega}), m_0(\boldsymbol{\omega} + \boldsymbol{\pi}_2), m_0(\boldsymbol{\omega} + \boldsymbol{\pi}_4), m_0(\boldsymbol{\omega} + \boldsymbol{\pi}_6)]^\top$ and V are the left singular vectors of $\mathfrak{D}(\omega)$ whose corresponding singular values are non-zero. If $\mathfrak{m}_0 \in span(V)$, then $\vartheta = 0$. If $\mathfrak{m}_0 \perp span(V)$, then $\vartheta = 1$. Fig.6 shows the feasibility check ϑ of input $\widetilde{m_i}(\boldsymbol{\omega})$, and $\mathfrak{m}_0$ is orthogonal to $span(V)$ everywhere.

6.2   solving $\widetilde{m_0}^C(\boldsymbol{\omega})$ and m_i

We compute $\widetilde{m_0}^C(\boldsymbol{\omega})$ by solving the following optimization problem similar to (21) for the dyadic scheme,

$$\min_{\mathbf{x}} \ \|\boldsymbol{D}(\mathbf{m}_0^C \circ \mathbf{x})\|^2 + \lambda \|\mathbf{w} \circ \mathbf{m}_0^C \circ \mathbf{x}\|^2, \quad s.t. \ A\mathbf{x} = \mathbf{1}, \ \mathfrak{D}\mathbf{x} = \mathbf{0} \quad (31)$$

where $\circ$ is Hadamard product and $\mathbf{w}$ is a weight vector and we consider real solution $\mathbf{x}$ here. A in the constraint is the matrix generated from the identity condition (16) and $\mathfrak{D}$ is generated from the singularity condition (24). Since A and $\mathfrak{D}$ are linearly independent, (31) is feasible. Here, instead of optimizing the
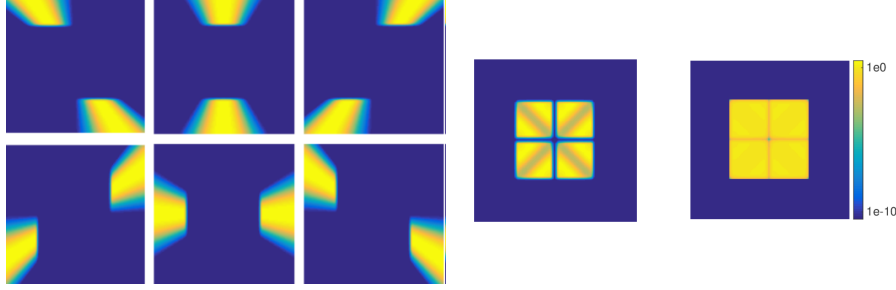
16

Figure 5: Left: $|\widetilde{m_i}(\boldsymbol{\omega})|$, middle: computed m_0^C, right: $\log(m_0^C)$
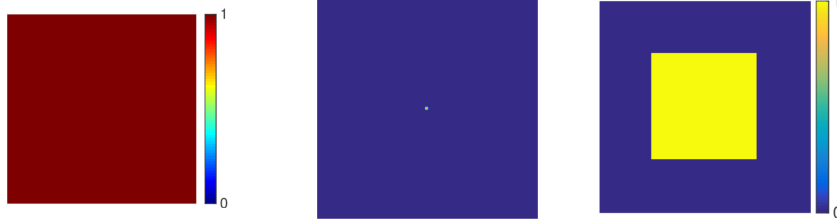

Figure 6: ϑ

Figure 7: Left: : computed $\widetilde{m_0}^C$, right: $\widetilde{m_0}^C \cdot m_0^C$

properties of $\mathbf{x}$ as in (21), we optimize those of $\widetilde{\mathbf{m}}_0^C \circ \mathbf{x}$ since $m_0^C \cdot \widetilde{m_0}^C$ will be later re-decomposed into m_0 and $\widetilde{m_0}$. In addition, if m_0^C is symmetric with respect to the two coordinates ω_x and ω_y, then we impose the same symmetry on $\widetilde{m_0}^C$ by solving (31) on $[0, \pi) \times [0, \pi)$ and then extend the solution to $[-\pi, \pi) \times [-\pi, \pi)$ by symmetry.

Fig.7 shows $\widetilde{m_0}^C(\boldsymbol{\omega})$ obtained from (31) and $\widetilde{m_0}^C \cdot m_0^C$ which is $\mathbf{1}_{S_1}$.

In particular, given $\widetilde{m_0}^C \cdot m_0^C = 1$, $\mathbf{b}(\boldsymbol{\omega}) = \mathbf{0}$, $\forall \boldsymbol{\omega} \in S_1$, hence $\mathbf{m}[2:7] = \mathbf{0}$. When $\mathbf{b}(\boldsymbol{\omega}) \neq \mathbf{0}$, (30) is a degenerated over-determinant linear system (we also do a sanity check here for the linearity between $\overline{\overline{\mathbf{M}}}[:, 2:7]$ and $\mathbf{b}$ by computing ϑ) and

$$\mathbf{m}[2:7](\boldsymbol{\omega}) = \left(\overline{\overline{\mathbf{M}}}[:, 2:7]\right)^{\dagger} \mathbf{b}(\boldsymbol{\omega}),$$

where $\dagger$ is the pseudo-inverse of a matrix. Fig.8 shows the solution m_i of (30) and the corresponding spatial filters $\mathcal{F}^{-1}\widetilde{m_0}$. As shown in Fig.8, the energy of m_i concentrates on $\{|\omega_x| = \frac{\pi}{2}, |\omega_y| = \frac{\pi}{2}\}$ where $|\widetilde{m_i}|$ is small, and the filters decay slowly in time domain.

The bi-orthogonal bases constructed is not ideal, despite the regularization on m_0 in the optimization (31). Since no explicit regularization is put on m_i, it's difficult to control the regularity of the output m_i from the input $\widetilde{m_i}$.
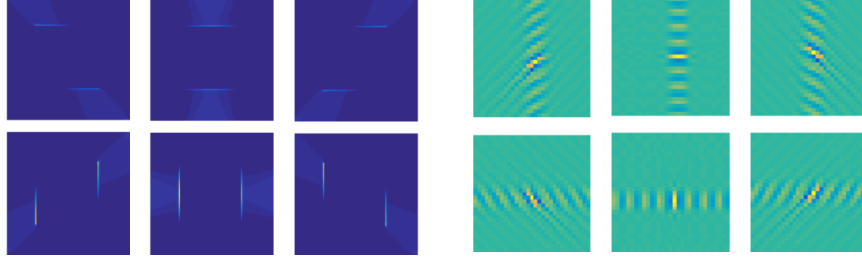
Figure 8: Left: $|m_i|$, $i = 1, \cdots, 6$, right:$|\mathcal{F}^{-1} m_i|$

7 Conclusion and future work

In this paper, we consider directional wavelet schemes on dilated quincunx sublattice and analyze their regularity. We show that filters in bi-orthogonal bases have the same discontinuity in the frequency domain as that of the orthonormal bases at the corners of $S_1 = [-\pi/2, \pi/2) \times [-\pi/2, \pi/2)$, hence they cannot be not well localized in the time domain.

We construct the bi-orthogonal taking a different approach from the orthonormal case, where directional dual filters are first designed such that they can be completed to a bi-orthogonal frame and the remaining filters are obtained by solving feasible linear systems or quadratic optimization. Its extension to low-redundancy dual frame construction is not studied here and will be our future focus.

Appendices

A   Proof of Theorem 1

Take the Fourier transform of both sides of (6), we have

$$\sum_{\boldsymbol{k}} \langle f, \phi_{\boldsymbol{k}} \rangle \hat{\phi}(\boldsymbol{\omega}) e^{-i\boldsymbol{\omega}^T \boldsymbol{k}} = \sum_{\boldsymbol{k}} \langle f, \phi_{1,\boldsymbol{k}} \rangle e^{-i\boldsymbol{\omega}^T \boldsymbol{D_2} \boldsymbol{k}} |\boldsymbol{D_2}|^{1/2} \hat{\phi}(\boldsymbol{D_2}^T \boldsymbol{\omega})$$

$$+ \sum_{j=1}^{J} \sum_{\boldsymbol{k}} \langle f, \psi_{1,\boldsymbol{k}}^j \rangle e^{-i\boldsymbol{\omega}^T \boldsymbol{D} \boldsymbol{k}} |\boldsymbol{D}|^{1/2} \hat{\phi}(\boldsymbol{D}^T \boldsymbol{\omega})$$

Suppose m_j are trigonometric series

$$m_0(\boldsymbol{\omega}) = \sum_{\boldsymbol{k}} c_{\boldsymbol{k}} e^{-i\boldsymbol{\omega}^T \boldsymbol{k}} \quad m_j(\boldsymbol{\omega}) = \sum_{\boldsymbol{k}} g_{\boldsymbol{k}} e^{-i\boldsymbol{\omega}^T \boldsymbol{k}}, \quad j = 1, \cdots, J \qquad (32)$$

The first term on the right hand side can be represented by $\hat{\phi}(\boldsymbol{\omega})$ and $\langle f, \phi_k \rangle$ using (1) and (32).

$$\text{the first term on R.H.S. } = \sum_{\boldsymbol{k}} \langle f, \phi_{1,\boldsymbol{k}} \rangle e^{-i\boldsymbol{\omega}^T \boldsymbol{D_2 k}} |\boldsymbol{D_2}|^{1/2} m_0(\boldsymbol{\omega}) \hat{\phi}(\boldsymbol{\omega})$$

$$= \sum_{\boldsymbol{k}} \Big(\sum_{\boldsymbol{k'}} \langle f, \phi_{\boldsymbol{k'}} \rangle \overline{c_{\boldsymbol{k'} - \boldsymbol{D_2 k}}} |\boldsymbol{D_2}|^{1/2} \Big) e^{-i\boldsymbol{\omega}^T \boldsymbol{D_2 k}} |\boldsymbol{D_2}|^{1/2} m_0(\boldsymbol{\omega}) \hat{\phi}(\boldsymbol{\omega})$$

$$= \sum_{\boldsymbol{k'}} \langle f, \phi_{\boldsymbol{k'}} \rangle \Big(|\boldsymbol{D_2}| \sum_{\boldsymbol{k}} \overline{c_{\boldsymbol{k'} - \boldsymbol{D_2 k}}} e^{i\boldsymbol{\omega}^T (\boldsymbol{k'} - \boldsymbol{D_2 k})} \Big) e^{-i\boldsymbol{\omega}^T \boldsymbol{k'}} m_0(\boldsymbol{\omega}) \hat{\phi}(\boldsymbol{\omega}).$$

Remark. If we have a shift $\boldsymbol{k}_0$ in the down-sample scheme, i.e. $\boldsymbol{D_2}\mathbb{Z}^2 - \boldsymbol{k}_0$ instead of $\boldsymbol{D_2}\mathbb{Z}^2$, so that we obtain coefficient of $\tilde{\phi}_{1,\boldsymbol{k}} = \phi_{1,\boldsymbol{k}+\boldsymbol{k}_0}$ instead of $\phi_{1,\boldsymbol{k}}$, and $\tilde{\phi}_1(\boldsymbol{x}) = \phi_1(\boldsymbol{x} - \boldsymbol{k}_0) = |\boldsymbol{D_2}|^{1/2} \sum_{\boldsymbol{k}} c_{\boldsymbol{k}} \phi(\boldsymbol{x} - \boldsymbol{k} - \boldsymbol{k}_0) = |\boldsymbol{D_2}|^{1/2} \sum_{\boldsymbol{k}} c_{\boldsymbol{k} - \boldsymbol{k}_0} \phi(\boldsymbol{x} - \boldsymbol{k})$. This change of down-sample scheme results in an extra phase term $e^{-i\boldsymbol{\omega}^T \boldsymbol{k}_0}$ in m_0. Here, we use the down-sample scheme without translation.

Since $\bigcup_{\boldsymbol{\beta} \in B} \{\boldsymbol{\beta}\} := \bigcup_{\boldsymbol{\beta} \in B}(\boldsymbol{D_2}\mathbb{Z}^2 + \boldsymbol{\beta}) = \mathbb{Z}^2$, where $B = \{(0,0), (1,0), (0,1), (1,1)\}$, the summation over $\boldsymbol{k'} \in \mathbb{Z}^2$ can be written as a double sum $\sum_{\boldsymbol{\beta} \in B} \sum_{\boldsymbol{k'} \in \{\boldsymbol{\beta}\}}$,

$$\sum_{\boldsymbol{\beta} \in B} \sum_{\boldsymbol{k'} \in \{\boldsymbol{\beta}\}} \langle f, \phi_{\boldsymbol{k'}} \rangle \sum_{\boldsymbol{k}} \overline{c_{\boldsymbol{k'} - \boldsymbol{D_2 k}}} e^{i\boldsymbol{\omega}^T (\boldsymbol{k'} - \boldsymbol{D_2 k})} e^{-i\boldsymbol{\omega}^T \boldsymbol{k'}} |\boldsymbol{D_2}| m_0(\boldsymbol{\omega}) \hat{\phi}(\boldsymbol{\omega})$$

$$= \sum_{\boldsymbol{\beta} \in B} \sum_{\boldsymbol{k'} \in \{\boldsymbol{\beta}\}} \langle f, \phi_{\boldsymbol{k'}} \rangle \sum_{\boldsymbol{k} \in \{\boldsymbol{\beta}\}} \overline{c_{\boldsymbol{k}}} e^{i\boldsymbol{\omega}^T \boldsymbol{k}} e^{-i\boldsymbol{\omega}^T \boldsymbol{k'}} |\boldsymbol{D_2}| m_0(\boldsymbol{\omega}) \hat{\phi}(\boldsymbol{\omega})$$

The summation over $\boldsymbol{k}$ in the middle is similar to the trigonometric form of m_0 in (32), but $\boldsymbol{k}$ takes value on the shifted sub-lattice $\{\boldsymbol{\beta}\}$ instead of $\mathbb{Z}^2$. Therefore, the summation equals to instead a linear combination of m_0 with shifts Γ_0,

$$\sum_{\boldsymbol{\pi} \in \Gamma_0} m_0(\boldsymbol{\omega} + \boldsymbol{\pi}) \, e^{i\boldsymbol{\beta}^T \boldsymbol{\pi}} = \sum_{\boldsymbol{k} \in \{\boldsymbol{\beta}\}} c_{\boldsymbol{k}} e^{-i\boldsymbol{\omega}^T \boldsymbol{k}} \tag{33}$$

Substitute (33) into the previous expression,

$$\sum_{\boldsymbol{\beta} \in B} \sum_{\boldsymbol{k'} \in \{\boldsymbol{\beta}\}} \langle f, \phi_{\boldsymbol{k'}} \rangle \sum_{\boldsymbol{\pi} \in \Gamma_0} \overline{m_0(\boldsymbol{\omega} + \boldsymbol{\pi})} \, e^{-i\boldsymbol{\beta}^T \boldsymbol{\pi}} \, e^{-i\boldsymbol{\omega}^T \boldsymbol{k'}} m_0(\boldsymbol{\omega}) \hat{\phi}(\boldsymbol{\omega})$$

Since $e^{i\boldsymbol{\pi}^T \boldsymbol{\beta}} = e^{i\boldsymbol{\pi}^T \boldsymbol{k'}}$, $\forall \boldsymbol{k'} \in \{\boldsymbol{\beta}\}$, after rewriting the double sum over $\boldsymbol{k'}$ back to a unit sum on $\mathbb{Z}^2$, we get

$$\sum_{\boldsymbol{k'}} \langle f, \phi_{\boldsymbol{k'}} \rangle e^{-i\boldsymbol{\omega}^T \boldsymbol{k'}} \hat{\phi}(\boldsymbol{\omega}) \Big(\sum_{\boldsymbol{\pi} \in \Gamma_0} \overline{m_0(\boldsymbol{\omega} + \boldsymbol{\pi})} m_0(\boldsymbol{\omega}) e^{-i\boldsymbol{\pi}^T \boldsymbol{k'}} \Big)$$

Similarly, the second term on the R.H.S. of (6) equals to

$$\sum_{j=1}^{J} \sum_{\boldsymbol{k'}} \langle f, \phi_{\boldsymbol{k'}} \rangle e^{-i\boldsymbol{\omega}^T \boldsymbol{k'}} \hat{\phi}(\boldsymbol{\omega}) \Big(\sum_{\boldsymbol{\pi} \in \Gamma_1} \overline{m_j(\boldsymbol{\omega} + \boldsymbol{\pi})} m_j(\boldsymbol{\omega}) e^{-i\boldsymbol{\pi}^T \boldsymbol{k'}} \Big)$$

(For Theorem 3 on frame construction, the summation of shifts $\boldsymbol{\pi}$ is over Γ_0 instead of Γ_1.) Combining the two terms on the R.H.S. of (6), and compare the coefficients of $\langle f, \phi_{\boldsymbol{k'}} \rangle e^{-i\boldsymbol{\omega}^T \boldsymbol{k'}} \hat{\phi}(\boldsymbol{\omega})$ on both sides, the perfect reconstruction condition is then equivalent to $\forall \boldsymbol{k'}$,

$$\sum_{\boldsymbol{\pi} \in \Gamma_0} e^{-i\boldsymbol{\pi}^T \boldsymbol{k'}} \overline{m_0(\boldsymbol{\omega} + \boldsymbol{\pi})} m_0(\boldsymbol{\omega}) + \sum_{j} \sum_{\boldsymbol{\pi} \in \Gamma_1} e^{-i\boldsymbol{\pi}^T \boldsymbol{k'}} \overline{m_j(\boldsymbol{\omega} + \boldsymbol{\pi})} m_j(\boldsymbol{\omega}) = 1.$$

This is equivalent to

$$|m_0(\boldsymbol{\omega})|^2 + \sum_j |m_j(\boldsymbol{\omega})|^2 = 1$$

and

$$\sum_{j=0}^{J} \overline{m_j(\boldsymbol{\omega}+\boldsymbol{\pi})} m_j(\boldsymbol{\omega}) = 0, \ \boldsymbol{\pi} \in \Gamma_0 \setminus \{\mathbf{0}\}$$

$$\sum_{j=1}^{J} \overline{m_j(\boldsymbol{\omega}+\boldsymbol{\pi})} m_j(\boldsymbol{\omega}) = 0, \ \boldsymbol{\pi} \in \Gamma_1 \setminus \Gamma_0$$

Remark. Because each m_j is $(2\pi, 2\pi)$ periodic, we only need to check the above equality $\forall \boldsymbol{\omega} \in S_0$. If we downsample ψ_1^j on a shifted sub-lattice $\boldsymbol{D}\mathbb{Z}^2 - \boldsymbol{k}_j$, we then have an extra phase $e^{i\boldsymbol{\pi}^T \boldsymbol{k}_j}$ before $\overline{m_j(\boldsymbol{\omega}+\boldsymbol{\pi})} m_j(\boldsymbol{\omega})$ in shift cancellation condition. This provides additional freedom in the construction yet it is not substantial.

B   Supplementary Numerical Results

B.1   Numerical optimization of $\widetilde{m_0}(\boldsymbol{\omega})$ in 1D

To test whether numerical optimization is a practical way to solve (19), we first experiment on $m_0(\omega)$ and $\widetilde{m_0}(\boldsymbol{\omega})$ of pre-designed bi-orthogonal wavelets. We consider a low frequency filters corresponding to bi-orthogonal scaling functions ϕ, $\tilde{\phi}$ with vanishing moments 3 and 5 respectively.

The filters are shown in Fig.9. Suppose we know the upper decomposition filter, and we want to find the lower reconstruction filter by solving (19), such that the filter has support as compact as possible. The corresponding m_0 and $\widetilde{m_0}$ are complex, yet we can shift the phase of m_0 such that m_0 is real and apply the same phase shift to $\widetilde{m_0}(\boldsymbol{\omega})$. Without loss of generality, (19) can be solved assuming that m_0 is real. It is not necessary that the corredponding $\widetilde{m_0}$ is also real, but in this testing case, $m_0(\boldsymbol{\omega})$ and $\widetilde{m_0}(\boldsymbol{\omega})$ have the same phase, hence the phase-shifted $\widetilde{m_0}(\boldsymbol{\omega})$ is real as well. Fig.10 shows the ground truth $m_0(\boldsymbol{\omega})$ and $\widetilde{m_0}(\boldsymbol{\omega})$ considered in this simulation.

Figure 9: 1d filters, up: LoD, down: LoR

Let $\widehat{\widetilde{m_0}}(\boldsymbol{\omega})$ be the approximation of $\widetilde{m_0}(\boldsymbol{\omega})$, which is solution of the following optimization problem

$$\min_{\mathbf{x}} \ \|\boldsymbol{D}\mathbf{x}\|^2 + \|\mathbf{x}\|^2, \quad s.t. \ \boldsymbol{A}\mathbf{x} = \mathbf{1} \tag{34}$$

where $\boldsymbol{A}$ in the constraint is the matrix generated from (16) (in 1D, only a single shift of π appears in the condition, so each row of $\boldsymbol{A}$ has two non-zero entries).
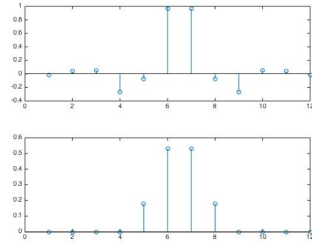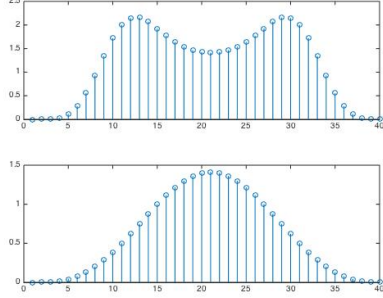
Figure 10: $m_0(\boldsymbol{\omega})$ and $\widetilde{m_0}(\boldsymbol{\omega})$ Figure 11: $\widehat{\widetilde{m_0}}(\boldsymbol{\omega})$ vs. $\widetilde{m_0}(\boldsymbol{\omega})$
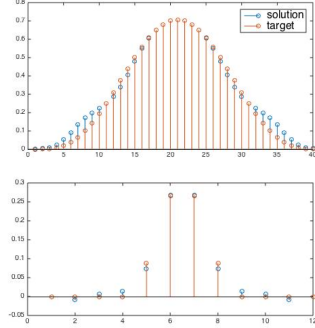
Notice that no symmetry constraint is imposed here, nevertheless, the solution shown in Fig.11 is almost symmetric. On the other hand, its support in the time domain is not as compact as that of $\widetilde{m_0}(\boldsymbol{\omega})$, see the bottom of Fig.11.

B.2   Numerical optimization of $\widetilde{m_0}(\boldsymbol{\omega})$ in 2D

The 2D case is much harder and several different optimization problems are formulated and their solutions are shown in the following. The 2D bi-orthogonal low-pass filters used here are the tensor products of the 1D filters used above. *2D version of* (34)

The 1D formulation can be easily extended to 2D, where $\boldsymbol{D} = [\boldsymbol{D}_x, \boldsymbol{D}_y]$ consider 1st order derivative in both x and y directions, and $\boldsymbol{A}$ is generated from (16), each row has four non-zero entries. Fig.12 shows the minimizer and compares it with the target function. It is obvious that the solution is not 90°-rotation invariant. Even worse is the fact that there is much energy in the vertical high-frequency domain.

Figure 12: Left: result of (34) in 2D, Right: target

To enforce the support of $\widehat{\widetilde{m_0}}(\boldsymbol{\omega})$ concentrates within the low frequency domain, the squared ℓ_2-norm regulator in (34) is changed to a weighted version (corresponding to Modulation space) as follows,

$$\min_{\mathbf{x}} \|\boldsymbol{D}\mathbf{x}\|^2 + \lambda\|\mathbf{w} \circ \mathbf{x}\|^2, \quad s.t. \ \boldsymbol{A}\mathbf{x} = \mathbf{1} \tag{35}$$

where $\circ$ is Hadamard product and $\mathbf{w}$ is a weight vector. In particular, we choose $\forall\omega, \ \mathbf{w}(\boldsymbol{\omega}) = \|\boldsymbol{\omega}\|$. Fig.13 and Fig.14 show the minimizer of (35) with $\lambda = 60$

and 600 respectively. As λ increases, the support of the minimizer concentrates more within the low frequency region. As shown in Fig.13, when λ is not huge, the minimizer achieves a certain level of but not full symmetry, whereas Fig.14 shows that huge λ imposes full symmetry.
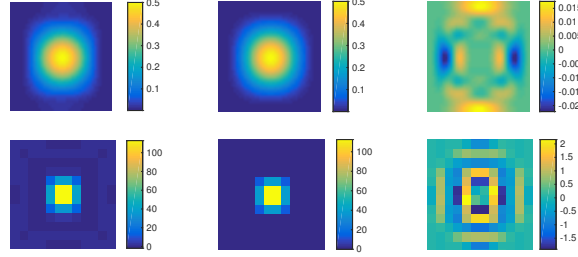

Figure 13: result of (35) $\widehat{\widetilde{m_0}}(\boldsymbol{\omega})$ ($\lambda = 60$), target $\widetilde{m_0}(\boldsymbol{\omega})$ and their difference, Top: frequency domain, Bottom: time domain
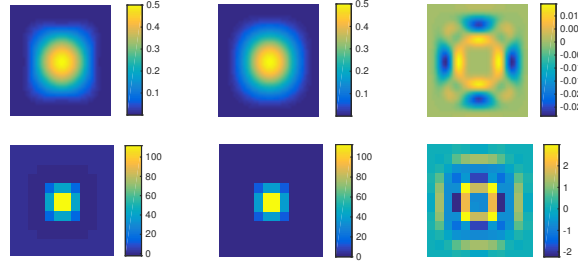
Figure 14: result of (35) $\widehat{\widetilde{m_0}}(\boldsymbol{\omega})$ ($\lambda = 600$), target $\widetilde{m_0}(\boldsymbol{\omega})$ and their difference

weighted L2 norm with symmetry constraint
If we hard constrain the symmetry by the following

$$\min_{\mathbf{x}} \ \|\boldsymbol{D}\mathbf{x}\|^2 + \lambda\|\mathbf{w} \circ \mathbf{x}\|^2, \quad s.t. \ \boldsymbol{A}\mathbf{x} = \mathbf{1}, \ \boldsymbol{S}\mathbf{x} = \mathbf{0} \tag{36}$$

where each row of $\boldsymbol{S}$ has an one entry and a negative one entry at the location of two points have the same value due to symmetry. In practice, we put symmetry constraints such that the upper half plane is symmetric to the lower half plane w.r.t. x coordinate and the first quadrant is $90°-$ rotational invariant w.r.t. the second quadrant. The symmetry constraint makes the optimization problem significantly harder, resulting in longer optimization algorithm running time and no near-optimal solution is found (the algorithm terminates as the maximum number of iterations is exceeded). Fig.15 shows the result provided by the Matlab quadratic minimization solver, unfortunately, there are artifacts at the near endpoints of x and y coordinates.

On the other hand, asymmetric solution can always be symmetrized by the average of the solution and its dual w.r.t. rotation, mirroring, etc. This approach
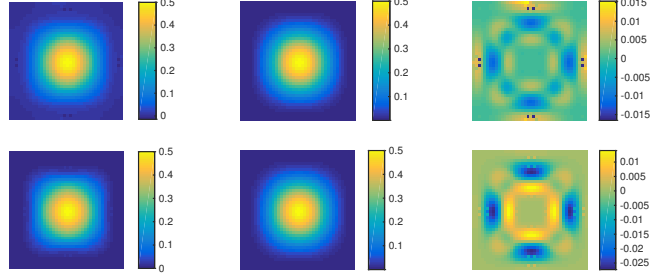
22

Figure 15: solution of (36) (top: $\lambda = 60$, bottom: $\lambda = 600$) provided by Matlab solver `quadprog`

increase the support of the solution, thus a well concentrated solution in the frequency domain is necessary to begin with.

Other potential formulations

We may also putting weights in the first L2-norm of derivatives, such that

$$\min_{\mathbf{x}} \ \|\mathbf{w}' \circ \boldsymbol{D}\mathbf{x}\|^2 + \lambda\|\mathbf{w} \circ \mathbf{x}\|^2, \quad s.t. \ \boldsymbol{A}\mathbf{x} = \mathbf{1} \tag{37}$$

Clearly, $\mathbf{w}'(\boldsymbol{\omega}) \to +\infty$ as $|\boldsymbol{\omega}| \to +\infty$, but its behavior near the origin is unclear.

References

[1] R. H. Bamberger and M. J. T. Smith, "A filter bank for the directional decomposition of images: theory and design," *IEEE Transactions on Signal Processing*, vol. 40, no. 4, pp. 882–893, Apr 1992.

[2] T. T. Nguyen and S. Oraintara, "Multiresolution direction filterbanks: theory, design, and applications," *IEEE Transactions on Signal Processing*, vol. 53, no. 10, pp. 3895–3905, Oct 2005.

[3] M. N. Do and M. Vetterli, "The contourlet transform: an efficient directional multiresolution image representation," *Image Processing, IEEE Transactions on*, vol. 14, no. 12, pp. 2091–2106, 2005.

[4] T. Sauer, "Shearlet multiresolution and multiple refinement." Kutyniok, Gitta (ed.) et al., Shearlets. Multiscale analysis for multivariate data. Boston, MA: Birkhäuser. Applied and Numerical Harmonic Analysis, 199-237 (2012)., 2012.

[5] G. Easley, D. Labate, and W.-Q. Lim, "Sparse directional image representations using the discrete shearlet transform," *Applied and Computational Harmonic Analysis*, vol. 25, no. 1, pp. 25–46, 2008.

[6] E. Candes, L. Demanet, D. Donoho, and L. Ying, "Fast discrete curvelet transforms," *Multiscale Modeling & Simulation*, vol. 5, no. 3, pp. 861–899, 2006.

[7] I. W. Selesnick, R. G. Baraniuk, and N. C. Kingsbury, "The dual-tree complex wavelet transform," *Signal Processing Magazine, IEEE*, vol. 22, no. 6, pp. 123–151, 2005.

[8] S. Durand, "M-band filtering and nonredundant directional wavelets," *Applied and Computational Harmonic Analysis*, vol. 22, no. 1, pp. 124 – 139, 2007.

[9] R. Yin, "Construction of orthonormal directional wavelets based on quincunx dilation subsampling," in *Sampling Theory and Applications (SampTA), 2015 International Conference on*, May 2015, pp. 292–296.

[10] A. Cohen and J.-M. Schlenker, "Compactly supported bidimensional wavelet bases with hexagonal symmetry," *Constructive approximation*, vol. 9, no. 2-3, pp. 209–236, 1993.

[11] A. Cohen, I. Daubechies, and J.-C. Feauveau, "Biorthogonal bases of compactly supported wavelets," *Communications on pure and applied mathematics*, vol. 45, no. 5, pp. 485–560, 1992.